

# **Ground improvement versus hybrid foundation and deep foundation – Comparison of foundation concepts for three case histories of European significance**

Univ.-Prof. Dipl.-Ing. Dr.techn. Dietmar ADAM  
Institute of Geotechnics, Vienna University of Technology  
Karlsplatz 13/220-2, A-1040 Wien, Austria  
e-mail: [dietmar.adam@tuwien.ac.at](mailto:dietmar.adam@tuwien.ac.at)  
Tel. +43-1-58801-22100, FAX +43-1-58801-22199

## **ABSTRACT:**

The focus of the keynote paper is on the comparison of different foundation concepts for three case histories of European significance.

The stadium in the Austrian city of Klagenfurt was designed and built for the EURO 2008 (Austria and Switzerland) in slightly consolidated soft lacustrine clays. The shallow foundation rests on floating stone columns installed with the vibro replacement technique allowing controlled large time-dependent settlements.

For the Combined Cycle Power Plant Malženice near Bohunice (Slovakia) a hybrid foundation concept was executed in collapsible aeolian silt deposits (loess). The ground was initially improved by the vibro replacement technique and the final cementation of the stone columns produced deep foundation elements.

The new spectacular cable-stayed bridge over the Sava River is the new landmark of Belgrade (Serbia). The 200 m tall pylon of the 965 m long bridge rests on a closed box foundation made of a clasping diaphragm wall and large-diameter bored piles inside. Thus, the highly concentrated loads are deeply transferred into the over-consolidated marls.

The different foundation concepts are compared and discussed. It is illustrated that all the concepts are justified taking into account the ground conditions, structural and serviceability requirements of the buildings, and economical factors (time and cost).

## **KEY WORDS:**

Ground improvement, hybrid foundation, deep foundation

## **1. EURO 2008 STADIUM KLAGENFURT (AUSTRIA)**

### **GROUND IMPROVEMENT CONCEPT**

#### **1.1. Introduction**

In 2008 the European Soccer Championship took place in Austria and Switzerland. Klagenfurt was one of the venues amongst others in Austria in particular in Salzburg, Innsbruck and Vienna. The new so called Wörthersee Stadium was situated near the centre of Klagenfurt in the vicinity of the Wörthersee, a large glacial lake in Carinthia. The project consists of the stadium oval with the integrated west building and three (temporary) canopied grandstands for 31,000 spectators. A new soccer academy building and a multifunctional gymnasium is directly connected to the oval. The stadium was designed in a way that the upper standings of the three grandstands can be deconstructed after the European Championship to a reduced size for 12,000 spectators. The characteristic form remains but the loads are significantly reduced.

Originally a bored pile foundation was designed for the west building due to the unfavourable ground conditions. Alternatively a shallow floating raft foundation on stone columns installed with the vibro replacement technique was executed. For the foundation of the girder and column structures of the three grandstands, the soccer academy building and the multifunctional gymnasium the ground was improved by stone columns as well as the ground beneath the highly loaded sections of the access ramp on the south west side of the stadium. Due to the unfavourable ground conditions settlements of about maximum 20 cm were predicted so that the deformation compatibility of the particular structures had to be carefully taken into consideration.

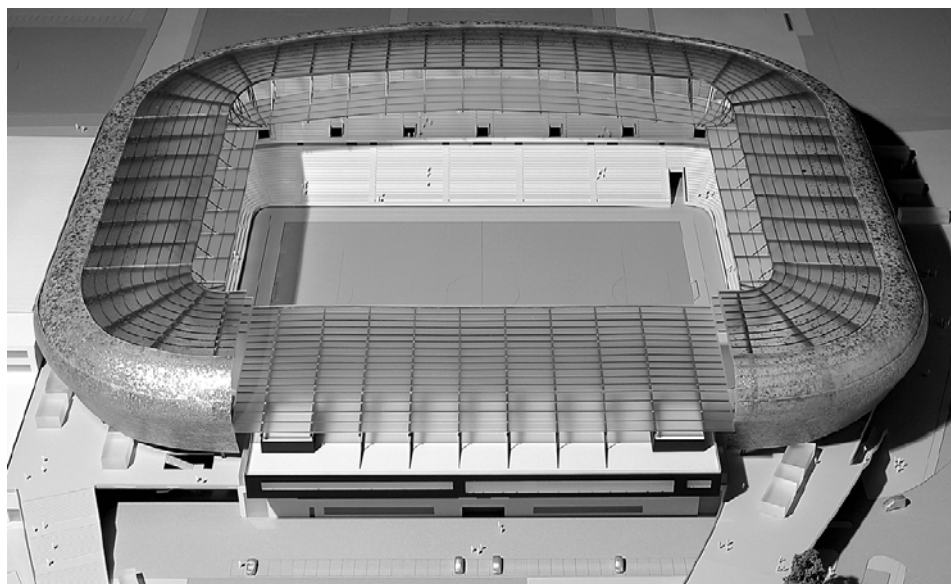


**Figure 1.** EURO 2008 Stadium Klagenfurt

## **1.2. Ground conditions**

Prior to construction ground exploration and soil investigation was performed in two phases. Rotational core drillings and dynamic probing heavy (DPH) and moreover,

seismic investigations to determine the interface between soft soil and bed rock revealed the following soil structure on the site of the stadium (Ingenieurgesellschaft Garber & Dalmatiner Zivilingenieure (2005a,b) and Bautechnische Versuchs- und Forschungsanstalt Salzburg (2006)):

Beneath the topsoil young unconsolidated sediments consisting of medium to coarse (gravelly) sands and silt (loam) are deposited up to a depth of 10 to 12 m below surface. Loose to medium dense sands predominate with increasing depth. These layers are underlain by young unconsolidated lake deposits consisting of medium dense silty fine sands followed by silty and clayey lake deposits up to 30 to 48 m beneath surface. Horizontally layered (very) soft clayey silts predominate and alternate with thin layers of silty fine sands and fine sandy silts. These lake deposits rest on sands and the ground moraine, the depth of the underlying bed rock consisting of sound quartz phyllite varies in a wide range below surface from about 31m in the north to about 60m in the south.

The groundwater table was explored in the drillings in a depth of about 2.3 m. The groundwater level fluctuates seasonally in a range of about 2.5 m in average. The groundwater is near the surface, thus influencing the soil conditions significantly.

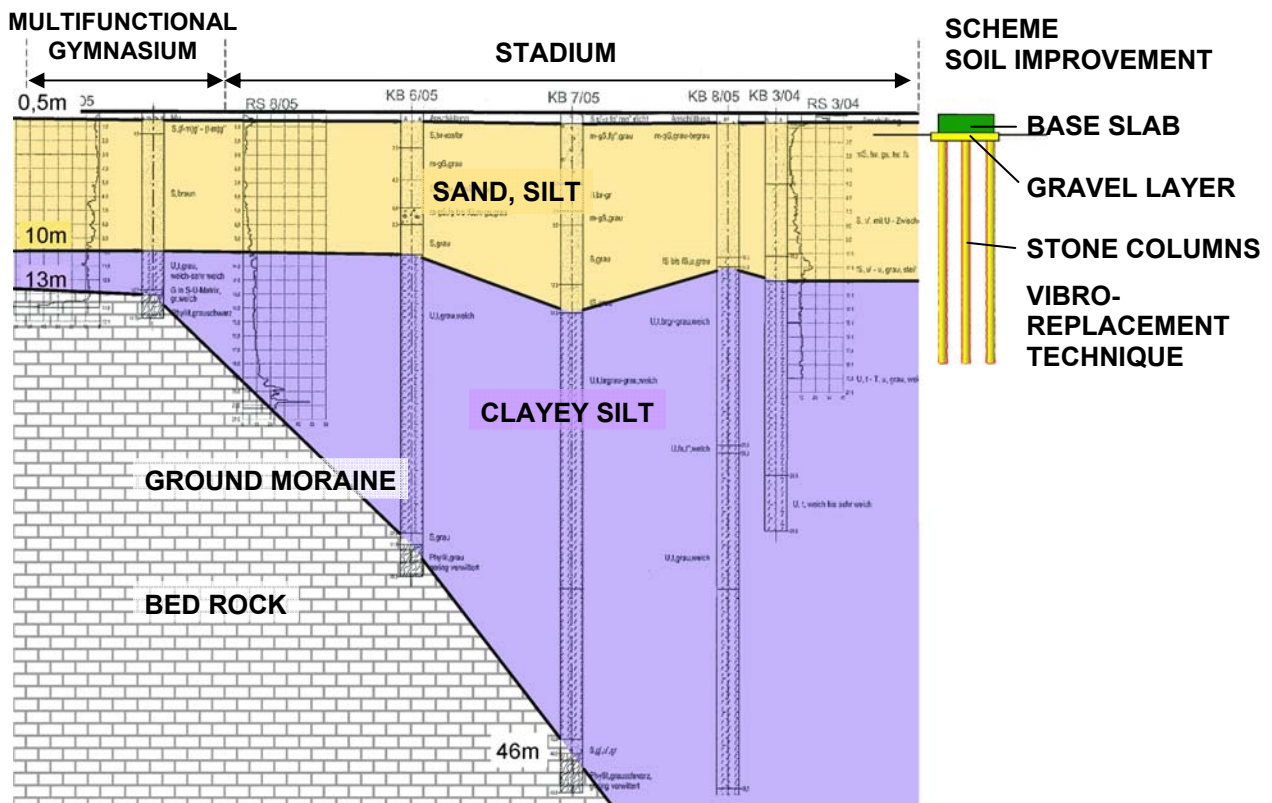


Figure 2. Ground conditions at the site of the stadium (schematic)

### 1.3. Ground improvement and foundation concept

Beneath all structures (west building, girder and column structures of the three grandstands, the soccer academy building and the multifunctional gymnasium, various single foundations) the ground was improved by installing stone columns and was thus prepared for the shallow foundations. The stone columns comprise a length of about 10 to 18 m below surface and were arranged taking into account the calculated foundation pressures and the soil interfaces found during installation. Thus, it was intended to homogenize the ground conditions on the one hand and to minimize the settlements and differential settlements on the other hand. Moreover, it was intended to accelerate the consolidation process in the ground through the highly permeable stone columns (Adam, 2008c).

In addition the liquefaction potential of the collapsible soil in the upper layers was reduced to increase the seismic soil resistivity in a case of an earthquake. This could be achieved by improving the shear parameters and increasing the overall permeability of the ground. Moreover, the compactable soil was improved around the stone columns by the vibratory installation process using the bottom feed vibrator technique. For drainage and load distribution a gravel layer was filled above the improved ground with varying thickness for the respective structure. The reinforced concrete slab of the west building was extended by a cantilever comprising a length of about 2 m in order to improve the pressure distribution due to the non-uniform loads beneath the raft foundation. Additionally, at the rear of the west building a preloading was applied to anticipate a specific portion of the expected settlements. Settlement measurements revealed that up to about 12 cm of settlements occurred from the preloading fill. Differential settlements between the west building and the adjacent (temporary) grandstands were taken into account by superelevating the raft foundation of the west building. In the area of the outer stairs in the northwest the soil was preloaded by a demolished building. The maximum allowable soil pressure was limited to 115 kN/m<sup>2</sup> since no deep ground improvement could be performed there. Soil exchange with recycled concrete aggregate was carried with a thickness of 100 cm. In the lower part of the access ramp in the southwest of the oval the ground was not improved.

The 10.5m high ramp adjacent to the west building was filled on ground improvement by stone columns for following reasons:

- Reduction of settlements to minimize deformations which could affect the west building;
- Acceleration of settlements by increasing the overall permeability of the ground to reduce the residual consolidation settlements to a minimum for the incorporated concrete structures, like transformer room, retaining walls and the bridge structure;
- Increase of shear strength of the soil to avoid local ground failure due to quick filling procedure;
- Providing sufficient safety against mechanical ground failure of structures which are incorporated into the ramp (especially the transformer room and the retaining structures).

A preloading in the front area of the ramp anticipated a considerable portion of predicted settlements. The preloading fill was removed after defined settlements occurred and the concrete structures were constructed. In defined areas of the multifunctional gymnasium with lower loads (playing field, access area) soil exchange was performed instead of stone columns. The base slab of the gymnasium was filled with concrete at the latest date after completion of the structure to minimize differential settlements between the structure and the base slab.

Ground improvement was checked by following test procedures:

- Dynamic probing heavy (DPH) before and after installation of stone columns to verify the improved properties of the ground;
- Dynamic load plate tests with the Light Falling Weight Device (LFWD) to check the bearing capacity and stiffness of the gravel fill layers and the exchange soil layers;
- Roller integrated Continuous Compaction Control (CCC) with vibratory rollers to check all fill layers and the formation layers of the foundations (e.g. raft foundation).

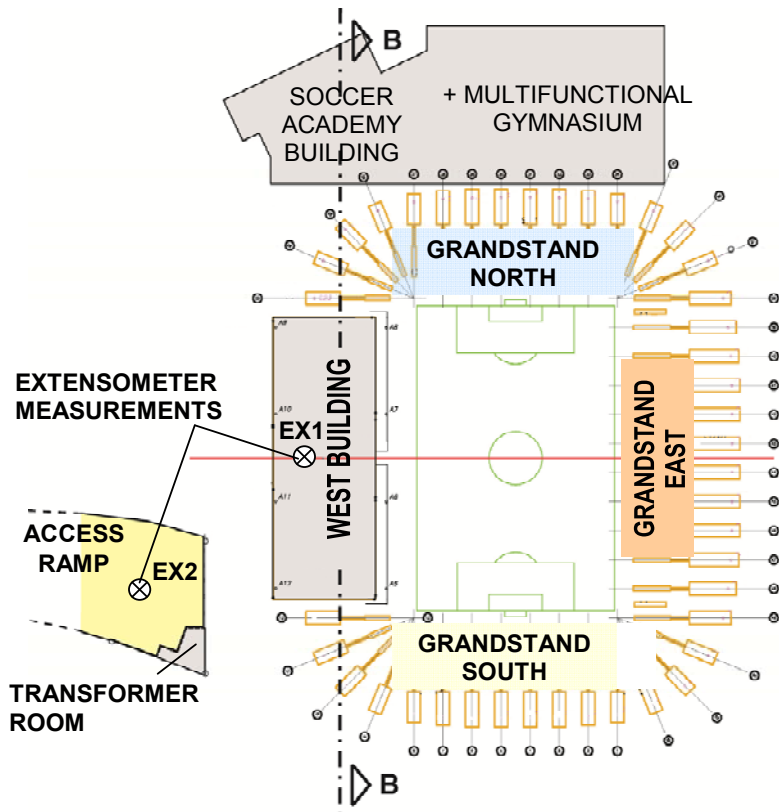


**Figure 3.** Layout of foundation scheme of several structures of the stadium.

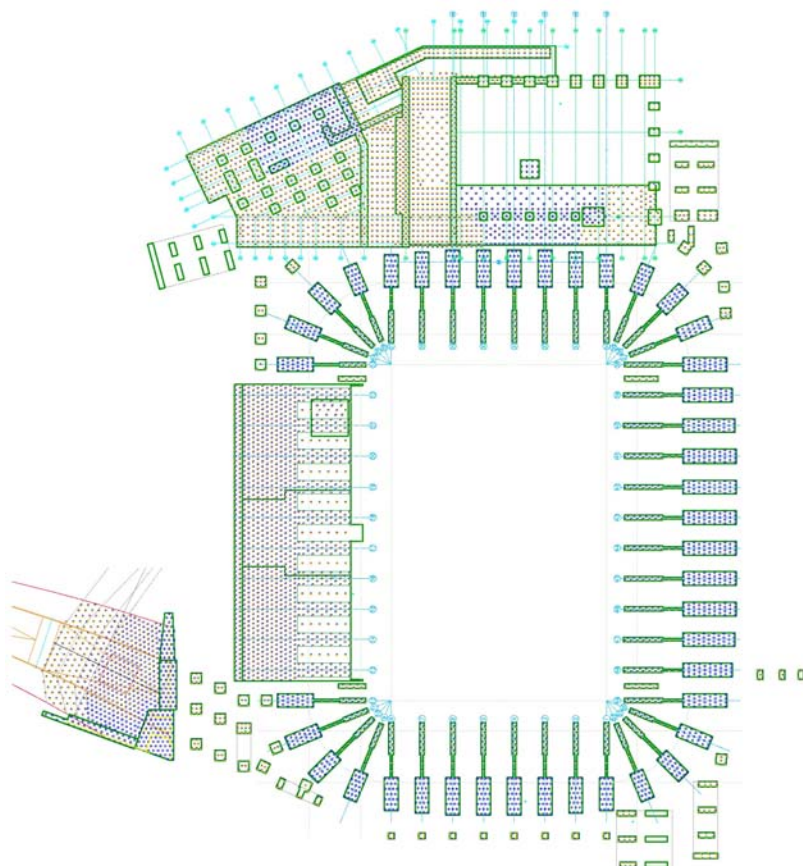


**Figure 4.** Layout of executed stone columns.

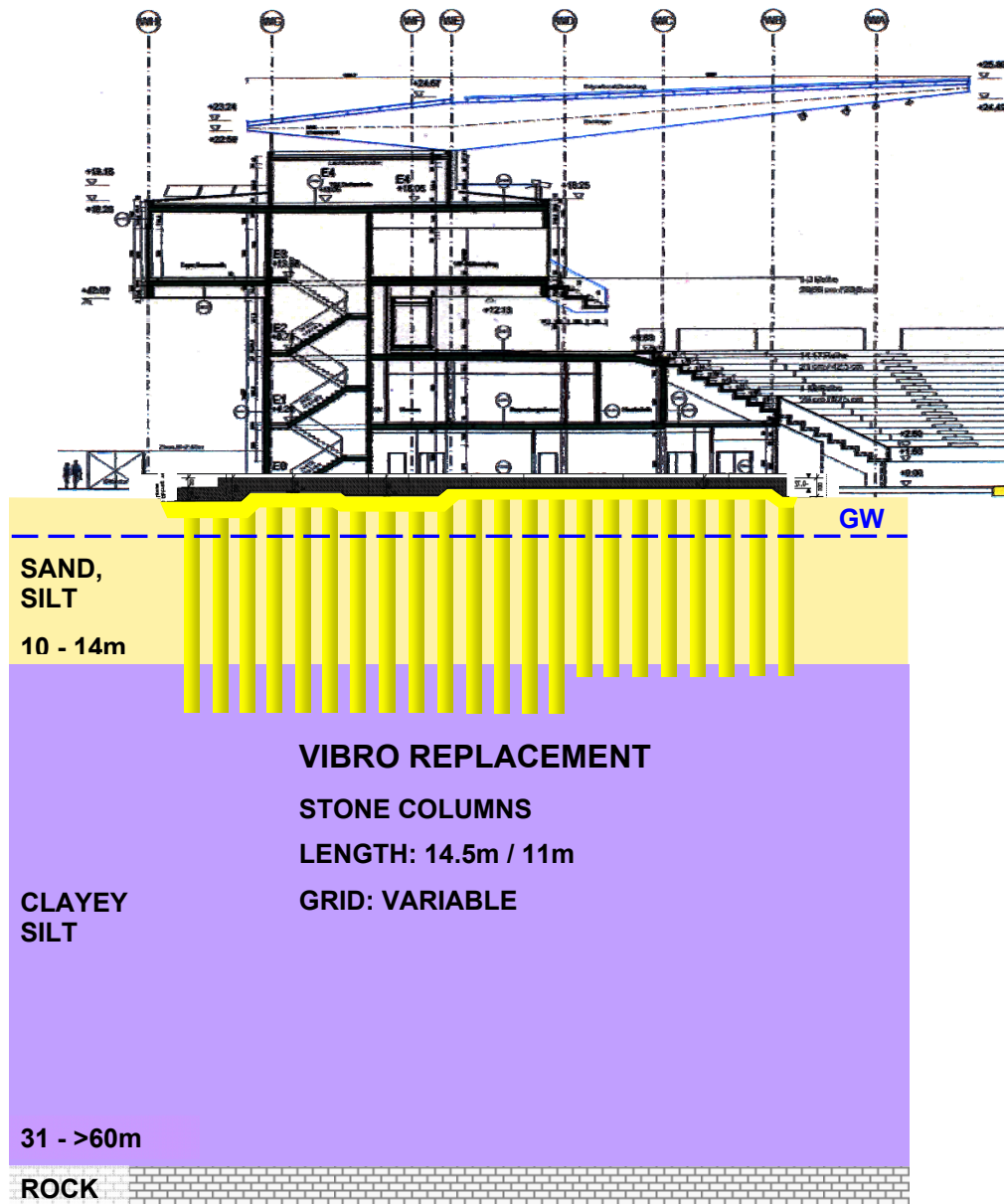


Figure 5. Cross section of the west building, raft foundation and stone columns.

#### 1.4. Prediction of settlement behaviour

The deep soil improvement with installed stone columns caused an increase of the bearing capacity of the ground, compaction of the soil by activating the self-compaction potential of the soil, a homogenization of the ground properties and an acceleration of consolidation settlements by increasing the overall permeability. Below the stone columns lake deposits comprise relatively homogeneous conditions but long-term settlements of about 3 to 6 cm after completion were predicted by the consolidation process and possibly by a creeping process as well. Due to the permeability and the stiffness of the soil it was assumed that the consolidation process will take some years.

In the design phase of the foundation concept settlement calculations were performed in order to predict the settlements and differential settlements for each building. In Table 1 the total settlements including the consolidation process are presented.

**Table 1:** Predicted settlements (expected values) for the west building taking into consideration soil improvement with stone columns and an extended slab (Adam, 2008c).

	s	$\Delta s$	length	inclination	
	[mm]	[mm]	[m]	[%]	[-]
corner SW	150	-	-	-	-
corner NW	130	-	-	-	-
corner NE	80	-	-	-	-
corner SE	90	-	-	-	-
outer side W	-	20	101	0.02	1/5050
side N	-	50	34	0.15	1/680
inner side E	-	10	101	0.01	<1/10000
side S	-	60	34	0.18	1/567

Settlement calculations revealed that settlements along the outer side in the west of the west building will be significantly larger compared to the inner side in the east because of the non-uniform load distribution. Moreover, the calculation results showed that the settlements in the north would be smaller than in the south of the west building. On the one hand the rock bed is not so deep below surface in the north than in the south and on the other hand the settlements of the access ramp affected the southern part of the west building as well. For this reasons an additional preloading fill was installed in the south of the west building.

The differential settlements within the west building were estimated to about 9 cm, nevertheless the derived angular rotation of the west building was within the limits. Thus, by means of the large dimensions the serviceability of the building was not affected by the differential settlements.

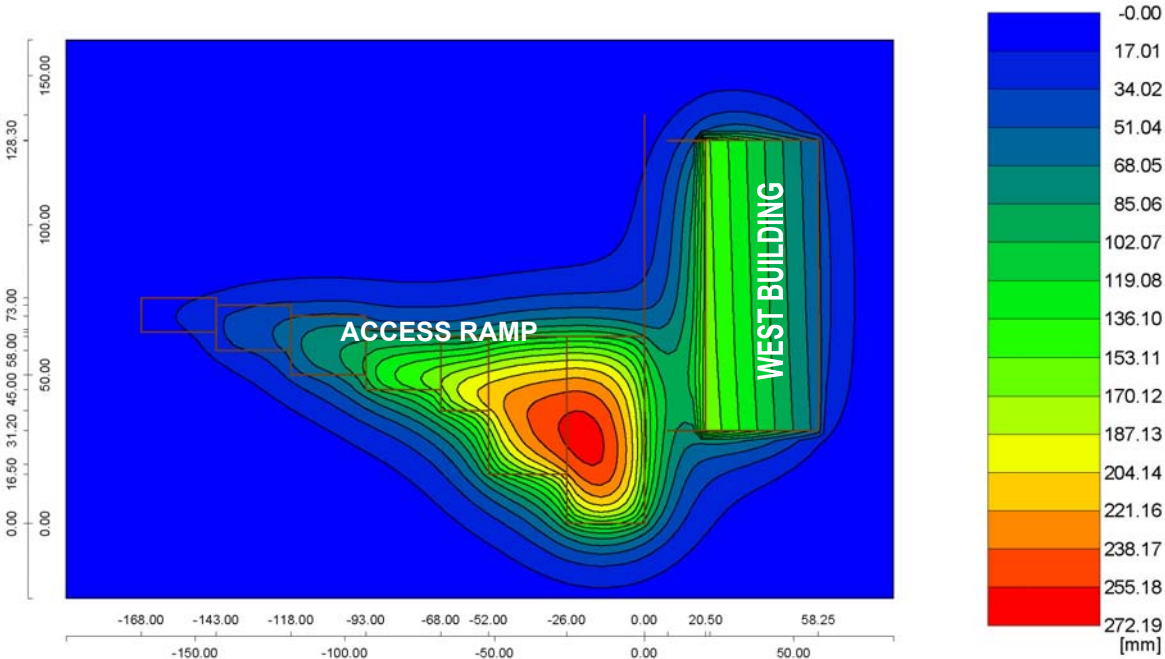


**Figure 6.** Calculated total settlements and determination of the mutual influence of west building and access ramp.

## 1.5. Monitoring of settlements

Settlement monitoring during the various construction sequences was performed in order to provide a continuous observation of the settlements of the ground. Measurement points for long-term settlement monitoring have been installed at the west building, the girder and column structures of the three grandstands, and the transformer building.

At the west building currently the settlements amount up to maximum 14 cm at the outer side (east) and up to maximum 7 cm (west). In comparison to the last settlement measurements a remarkable increase of the settlements was observed in the south western corner of the stadium.

Results of the progress of settlements over time reveal that the outer and the inner sides of the west building settle unequally. In the period from March 2007 to December 2009 (about 33 months) the inner side settled for about 1.5 cm while the outer side settled for about 7 cm. Moreover, the south western corner (about 7 cm) is stronger affected by the ramp than the north western corner (about 5.5 cm). As expected the settlements are influenced by the superposition of the deformations of the west building and the ramp.

Progress of settlements over time and the evaluation according to Sherif (ÖNORM B 4431-2) show that the settlements decay already at the inner side but until now not at the outer side. According to the evaluation according to Sherif about 80% of the total settlements occurred so that about 20% are still to be expected in the future.

In spite of the differential settlements between the outer and the inner side of the west building the maximum gradient of the VIP box in the upper floor is in a range of about 0.2% according to the measurements. Thus, the serviceability of the building is not affected by the differential settlements.

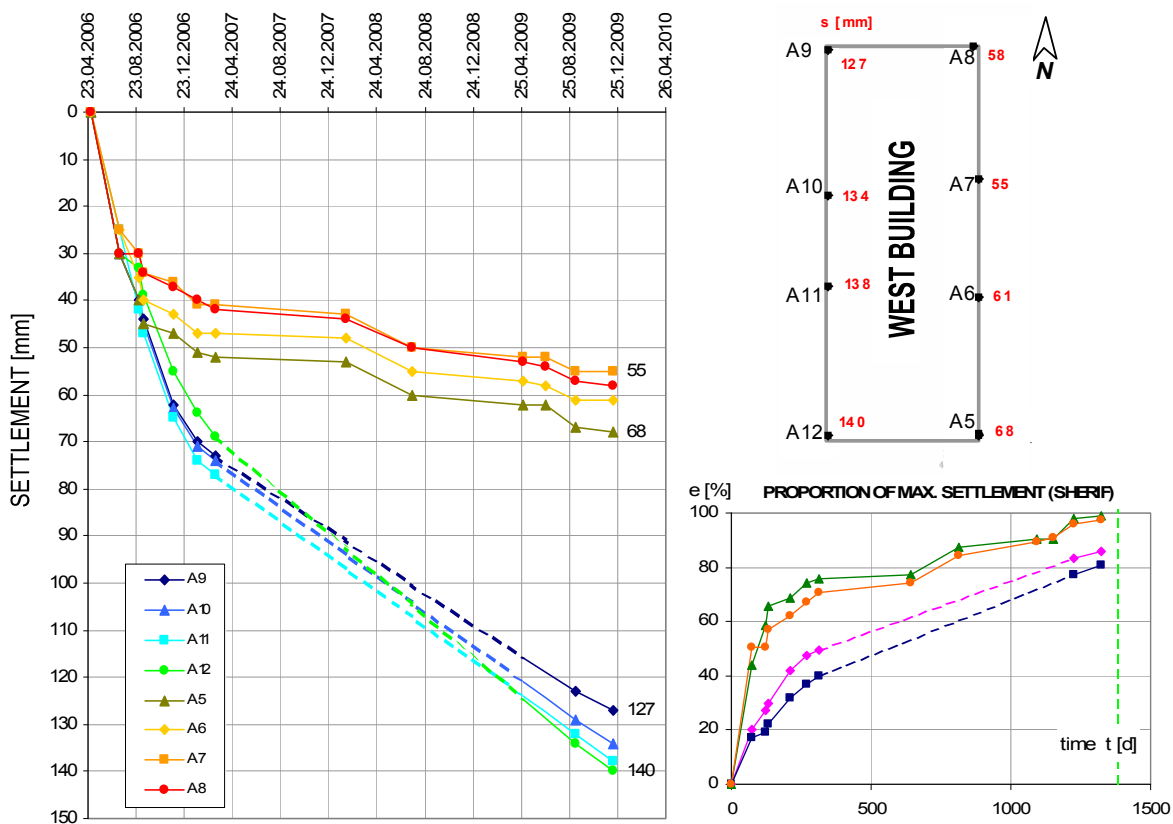


**Figure 7.** Geodetic settlement measurements for the west building, position of the measurement points and prediction of final settlements according to Sherif.

The differential settlements at the girder and column structures of the three grandstands are in a range from 0 to 0.8 cm. Only between the structures G11 and G12 and between G23 and G24 adjacent to the west building the differential settlements are larger as expected due to the influence of the west building. However, different deformations can be taken into account by readjusting the tension rods of the bracings. Differential settlements are limited to 2 cm only at foundations of girder and column structures with fixed bracings consisting of tension and pressure rods (so called K bracings). Actual measured values are however far below this limit values.

Settlement measurements show that total settlements have only marginally increased. However, it is expected that certain additional consolidation settlements occur.

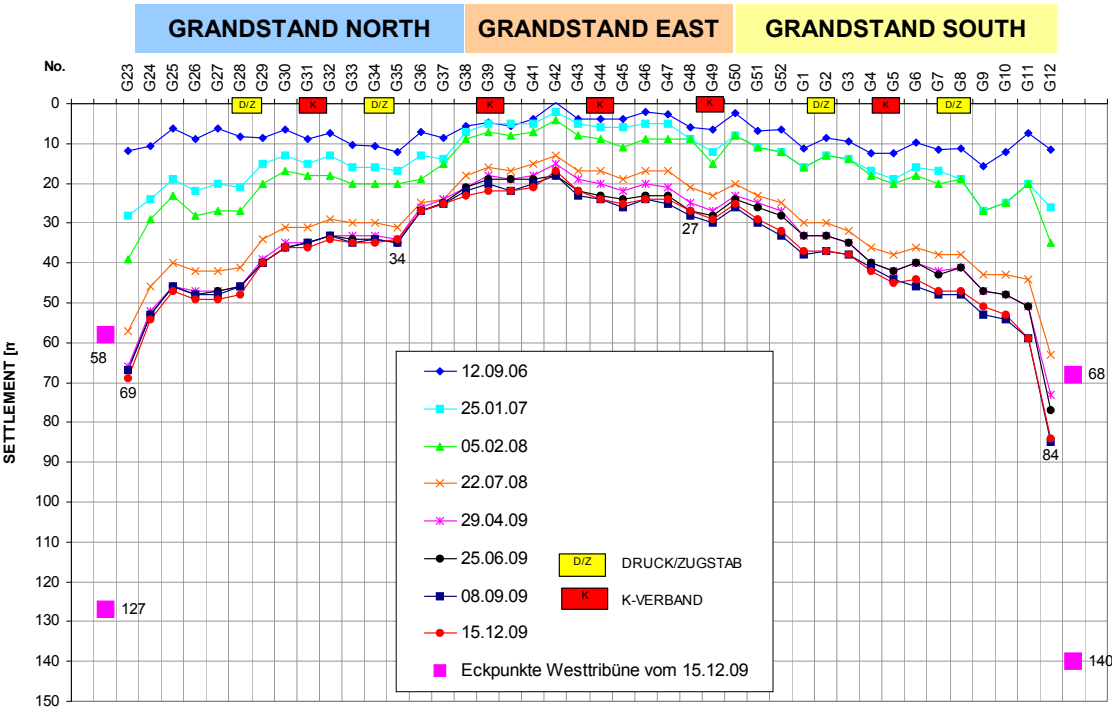


**Figure 8.** Settlements over time at the girder and column structures of the three grandstands.

Measured total settlements at the ramp show maximum values of about 18 cm. By means of the influence of the west building additional settlements occur at measure point SP34. Additional settlements at measure point SP36 are caused by the loads on all sides and the extensive settlement influence of the access ramp. The prediction of the final settlements according to Sherif has revealed that about 80% of the total settlements have occurred up to the present.

In a large scale well instrumented field trial consisting of multilevel-piezometers, multilevel-extensometers and earth pressure cells as well as a horizontal inclinometer the performance of the floating stone column foundation was investigated. The measurements give valuable insight into the installation process of stone columns and the evolution of pore water pressures and settlements over time beneath the 10.5 m high access ramp (Gäb et al., 2007). In Figure 11 results of extensometer and multilevel-piezometer measurements are presented revealing the effect of increasing the over-all permeability in the zone of the stone columns. Pore water pressures decrease rapidly after completion of stone columns installation thus accelerating consolidation settlements in the ground. Below the stone columns the permeability of the ground is low so that pore pressure and consolidation settlement take a long time presumably some years.

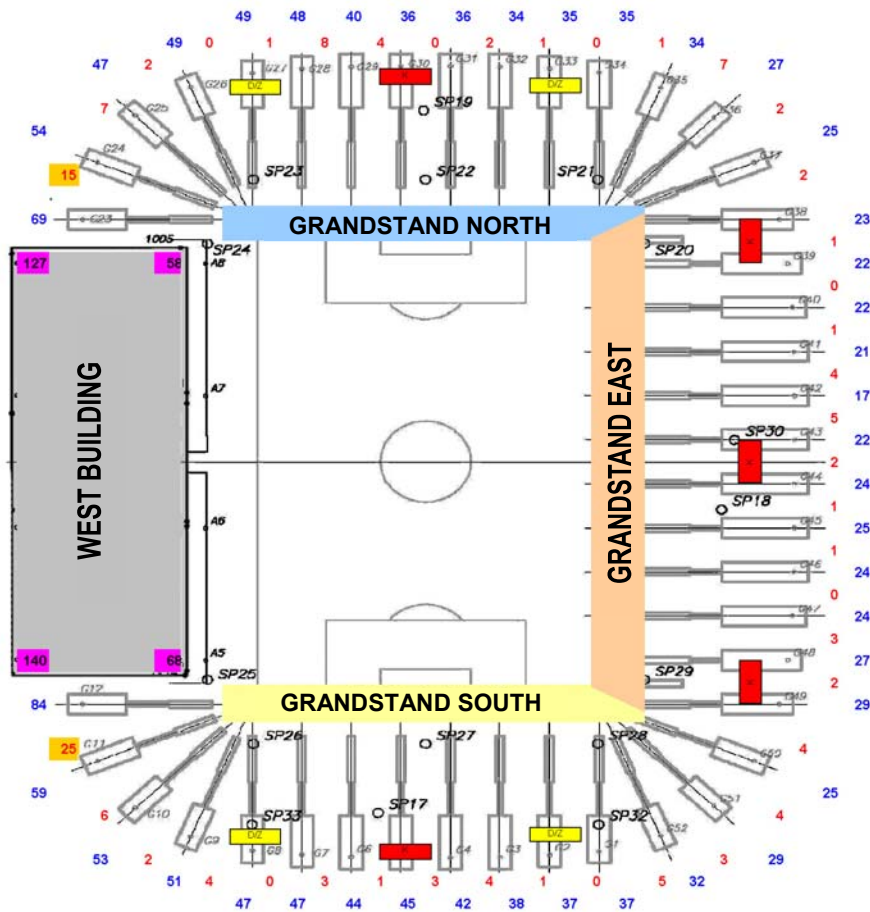


**Figure 9.** Geodetic settlement measurements (blue; unit: mm) and differential settlements (red; unit: mm) between the girder and column structures of the three grandstands; measurement campaign of December 2009.

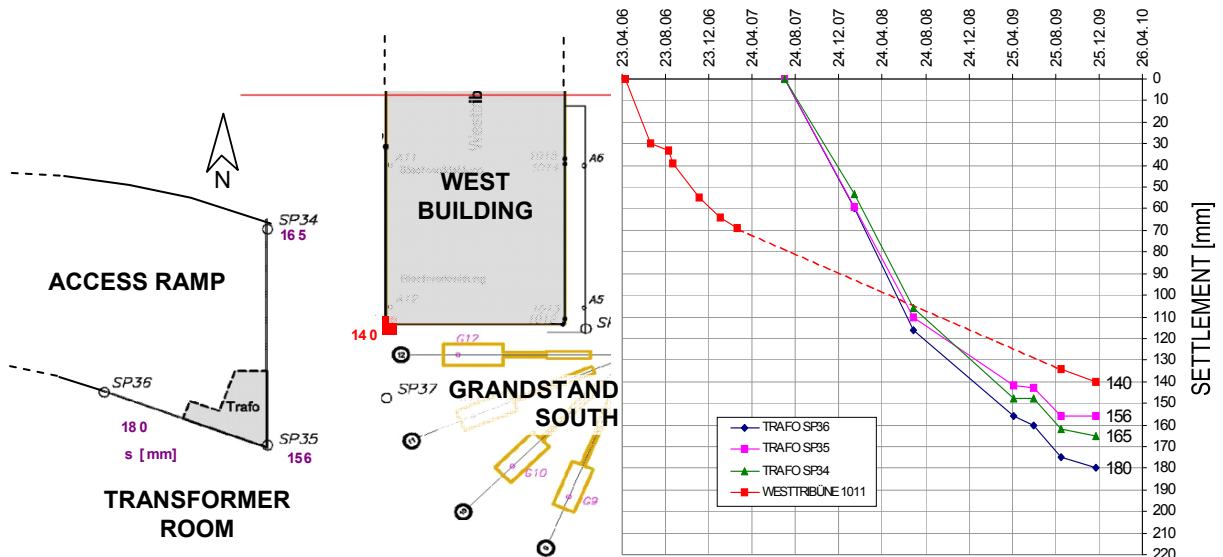


**Figure 10.** Geodetic settlement measurements (blue; unit: mm) and differential settlements (red; unit: mm) between the girder and column structures of the three grandstands; measurement campaign of December 2009.

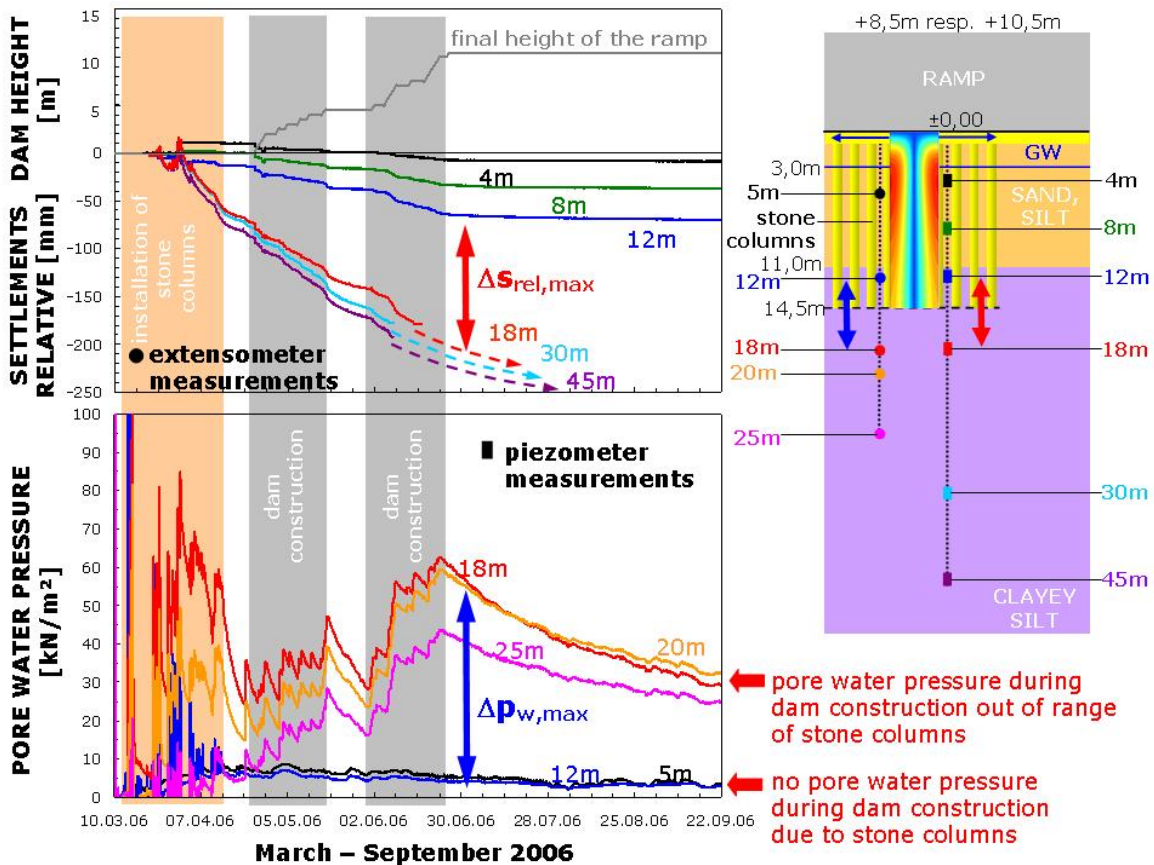


**Figure 11.** Results of the large scale field trial to investigate the performance of the floating stone columns foundation beneath the access ramp (Gäb et al., 2007).

## 1.6. Back analysis of settlements of the west building

A series of finite element analyses have been performed for this project and comparison of field measurements with 2D analyses employing different constitutive models has been presented in (Gäb et al., 2008) for the heavily instrumented trial field set up in the area of the ramp. Thus these results will not be repeated here but results from back analysis of the settlement behaviour of the west building will be discussed in the following. In addition to the settlement measurements shown in Figure 9 an extensometer has been installed at the west building (location see Figure 3) and these measurements will be considered too.

### 1.6.1. Short description of numerical and constitutive models

Considering the ground conditions a 3D model would be required to capture the inclined layers of soil in detail. However, for this preliminary study a cross section through the middle of the west building is taken postulating plane strain conditions (see Figure 12). The stone columns are modelled as “walls” with depths of 14.5 m on the left side and 10.5 m on the right side respectively. The space between the stone columns is 0.9 m. Figure 12 also shows the different soil layers according to Figure 2. It is noted that for simplicity the layers are assumed as horizontal. The rock (quartz phyllite) is not modelled, because its influence on the settlement behaviour can be considered negligible. Around the stone columns a zone is introduced in which the material properties have been adjusted. In this sand layer (“Sand dense”) the

stiffness has been increased due to significant compaction of the originally loose sand during the installation of the columns.

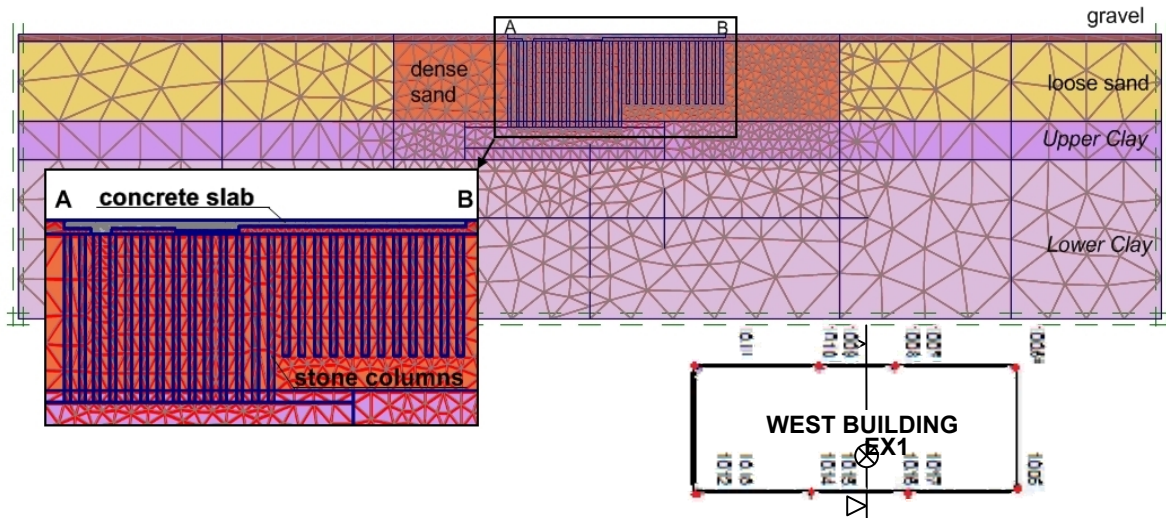


**Figure 12.** Cross section and 2D numerical model.

The Soft Soil Creep model (SSC) is used for this study which is an extension of the so-called Soft Soil model, both available in model library of the finite element code Plaxis (Brinkgreve et al., 2006). The Soft Soil Creep model is based on the approach proposed by Bjerrum(1967) and Janbu(1967) and considers time and strain rate effects. Thus the total strain consists of a time independent elastic part and a time dependent visco-plastic part. The creep effects are introduced by the modified creep index  $\mu^*$ , which is related to the creep index  $C_{\alpha}$ . The constitutive parameters required for the SSC model are the modified compression index  $\lambda^*$ , the modified swelling index  $\kappa^*$ , the modified creep index  $\mu^*$ , the friction angle  $\phi'$ , cohesion  $c'$ , dilatancy angle  $\psi$ , Poisson's ratio  $\nu$  and coefficient of earth pressure at rest  $K_{0,nc}$ . These parameters can be determined by standard triaxial and oedometer tests. A detailed description of the model can be found in (Vermeer and Neher, 2000). The Soft Soil Creep model is used for the clayey silt layers, for all other soil layers and the stone columns the Plaxis Hardening Soil model (Brinkgreve et al., 2006) is used. The parameters are summarized in Table 2.

**Table 2:** Material parameters for soil layers

	$k_x$	$k_y$	$\gamma$	$\gamma$	$c$	$\phi$	$\psi$	$\nu$	$\kappa^*$	$\lambda^*$	$\mu^*$		OCR	$K_{0,nc}$
	[m/s]	[m/s]	[kN/m <sup>2</sup> ]	[kN/m <sup>2</sup> ]	[kN/m <sup>2</sup> ]	[°]	[°]	[-]	[-]	[-]	[-]		[-]	[-]
Upper Clay	2.6E-9	7.9E-9	16	19	10	22.5	0	0.2	0.0053	0.028	0.0009		1.3	0.617
Lower Clay	2.4E-8	2.3E-7	16	19	10	22.5	0	0.2	0.005	0.026	0.00085		1.3	0.617
	$k_x$	$k_y$	$\gamma$	$\gamma$	$c$	$\phi$	$\psi$	$\nu$	$E_{50}^{ref}$	$E_{oed}^{ref}$	$E_{ur}^{ref}$	$m$	OCR	$K_{0,nc}$
	[m/s]	[m/s]	[kN/m <sup>2</sup> ]	[kN/m <sup>2</sup> ]	[kN/m <sup>2</sup> ]	[°]	[°]	[-]	[MN/m <sup>2</sup> ]	[MN/m <sup>2</sup> ]	[MN/m <sup>2</sup> ]	[-]	[-]	[-]
Loose sand	1E-5	1E-5	18	21	0.1	27.5	2	0.2	16	16	80	0.55	1	0.538
Dense sand	1E-5	1E-5	18	21	0.1	27.5	2	0.2	40	40	120	0.65	1	0.538
Stone columns	1E-5	1E-5	20	23.5	0.1	35	5	0.2	250	25	75	0.3	1	0.426
Gravel	1E-5	1E-5	20	20	0.1	35	0		35	35	105	0.5	1	0.426
Concrete slab	-	-	25	-	-	-	-	0.2	3E7	-	-	-	1	-

## 1.6.2. Results

Results from the numerical back-analysis are compared to the measurements of points (1007/1008 (A10) - 1009/1010 (A11) and 1014/1015 (A6) - 1016/1017 (A7)) according to Figure 13. These data correspond to the simulated vertical displacement of points A and B (Figure 12). Furthermore, available extensometer measurements (EX1) are taken into consideration. The results for vertical displacements versus time are illustrated in Figure 13. The calculated vertical displacements in point A agree very well with the measurements of 1007/1008 and 1009/1010. Also the measurements obtained from the extensometer in 4 and 8 m depth can be reproduced very well. However, vertical displacements in point B are too high compared to measured values. The reason for this discrepancy is not yet clear and needs further investigations. It is likely that the load in this section has been overestimated.

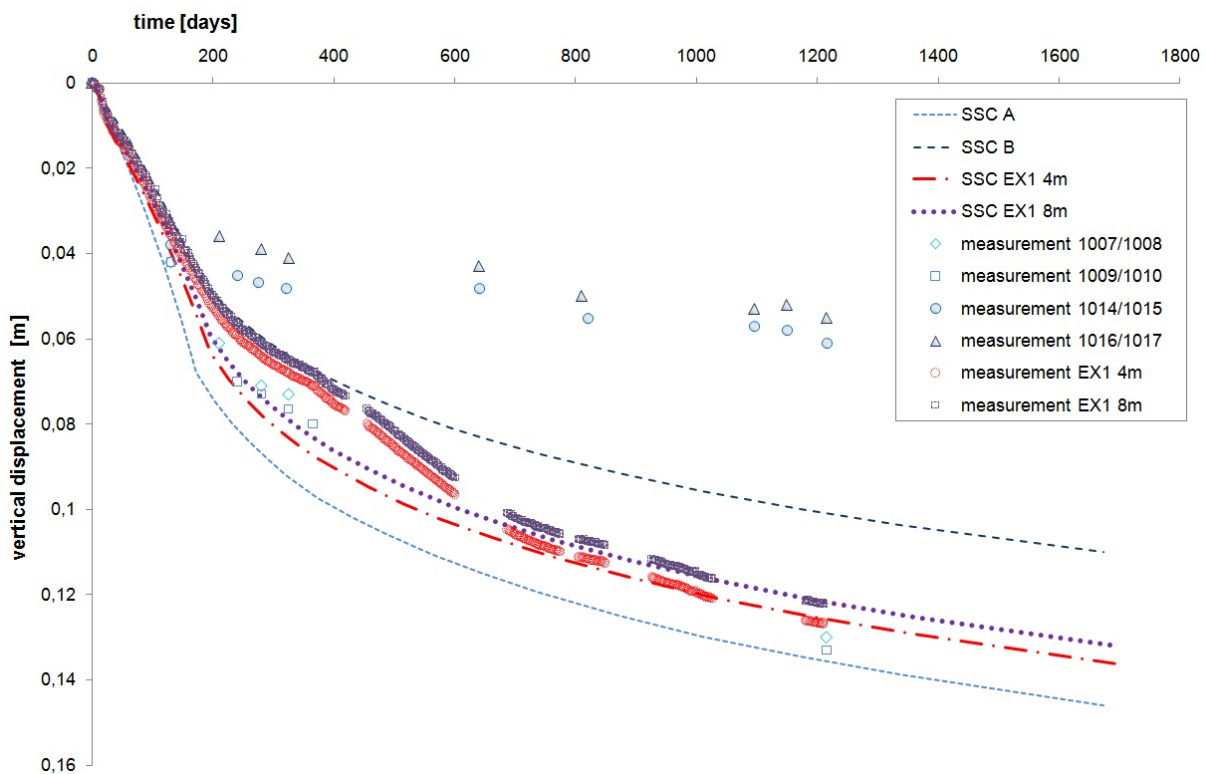


**Figure 13.** Results of back-calculation using SSC model: vertical displacements.

## 2. CCPP MALŽENICE (SLOVAKIA)

### HYBRID GROUND IMPROVEMENT AND DEEP FOUNDATION CONCEPT

#### 2.1. Introduction

E.ON Elektrárne, s.r.o., SPP Kompresorová stanica 3, SK-919 33 Trakovice, the in Trakovice based subsidiary of E.ON Kraftwerke GmbH in Hannover, Germany, erected a 400 MW gas fired combined cycle power plant (CCPP) at Malženice, in the western part of Slovakia, roughly 60 km north east of the capital Bratislava. The E.ON Elektrárne s.r.o. plant has been designed as a combined cycle power plant with an efficiency of 58% resulting from the combination of a gas turbine system and a

steam turbine system and supplies over 600,000 households with electricity, efficiently and reliably throughout the whole year. The power plant is fuelled by environmentally friendly natural gas. The cooling water is taken from the river Dudvah. Commercial operation of this gas power station started in 2012.

The investor and operator of the Malženice gas and steam turbine power plant is the in Trakovice based E.ON Elektrárne s.r.o. SIEMENS AG from Germany was appointed as general contractor. Civil construction works were carried out by the consortium Porr & Alpine Mayreder from Austria. On behalf of the consortium Porr & Alpine Mayreder, the civil design works were done by the Austrian offices Zorn & Nowy ZT GmbH, Heindl & Partner ZT GmbH and Convex ZT GmbH.

The developed foundation concept, based on a detailed investigation of the ground conditions at the site of the planned CCPP, combines stabilization of the soil beneath the base slab of the structures of the planned CCPP (ground improvement) and the vibro replacement technique to produce pile-like bearing elements in the form of stone columns and grouted stone columns and to improve the soil deeply (deep foundation and deep soil improvement). This innovative hybrid foundation concept is presented in the following.



**Figure 14.** Visualisation of the planned gas fired combined cycle power plant (CCPP 400 MW) at Malženice, in the western part of Slovakia, roughly 60 km North East of the capital Bratislava.

## 2.2. Ground conditions

According to the geomorphologic classification the area belongs to the Danube lowlands region, the Danube plain entity, the subdivision of Trnavská pahorkatina (hilly area) and the part of Trnavská tabula's (tableland). Topography of the area is plane, with the gentle depressions which were formed by the local steam pattern. The altitude above sea level is varying between about 166 to 168 m a.s.l. (m B.).

From the geological point of view the area at issue is part of the Danube Neogene's basin which started to take shape in the Upper Badenian. The older neogene series of strata occur at the peripheral parts of the basin in the broader area of interest. The uppermost neogene series of strata of Dacian and Rumanian which is widespread in the Trnavská pahorkatina (hilly area) are lying discordantly over the variegated Pontian. Lithological development of the sediments of Dacian and Rumanian is considerably variable. The latter are most frequently represented by gravelly-sandy sediments and by the strata of clays and strongly clayey gravels. Quaternary is built up of aeolian and fluvial sediments. Aeolian sediments are represented by loess (corresponding to clays of low plasticity), the thickness of which varies depending on morphology of the sub-base. The loess was blown in Pleistocene on the already modelled surface of hilly area. They are of light-yellow to light-brown colour, considerably monotonous, with sporadic content of the fine sand. They often include the calcareous concretions of size of chiefly 1-2 cm, sporadically however even larger. Calcium carbonate imparts the loess stability which manifests itself by a typical vertical jointing. Among characteristics of loess belongs also collapsibility. In the deeper horizon increases the amount of clayey fraction.

Almost the entire area is covered on the surface by the loess which, from the point of view of groundwater occurrence, are significant. Under the loess occurs the gravelly-sandy complex of strata of Upper Pliocene and the Quaternary, probably alluvium of river Váh which is well water-saturated. It is represented by gravels and sands which in particular in horizontal direction frequently alternate. The thickness of the water-saturated complex of strata is several meters.

The gravelly-sandy series of strata forms the vast groundwater reservoir with unconfined as well as confined water level. Groundwater resources of the gravelly-sandy aquifer are recharged by the infiltration of precipitation water from the region of Malé Karpaty (Little Carpathian Mts.) and by the infiltration from the water sources which are locally cut down into the gravelly-sandy sediments.

In detail the ground conditions at the site of the planned power plant have been explored in summer 2008. The results and conclusions of geological investigations carried out in the past in vicinity of the interesting area were also taken into account. The soil investigations comprised field investigations in the form of exploration pits, core drillings, standard penetration tests in the boreholes (SPT), dynamic probing heavy (DPH), penetration tests (CPT) and crosshole seismic measurements, and soil mechanical and chemical laboratory tests. Main findings regarding stratigraphy and soil conditions are concluded in the following.

Agriculture soil, anthropogenic backfills and fills (layer complex A) have been found up to a depth of about 1 m below the ground level of the nearly horizontal site (top between about 167 m and 168 m B.).

Below the explored anthropogenic backfills and fills, provided that won't reach deeper, occur the aeolian sediments in the form of loess and loess loams (layer complex B) up to about 14 m to 16 m b.g.l. (Note: m b.g.l. = meter below ground level). Sandy-clayey silt with medium plasticity and lime concretions up to 40 mm prevail in the lower horizon. In the transition zone to the beneath alluvial sediments sandy, stiff to very stiff clay with lime concretions up to 80 mm have been explored. The loessoid soil complex can be subdivided on the basis of macroscopic evaluations, laboratory tests and penetration tests into several horizons.

The 1<sup>st</sup> loess horizon consists of aeolian sediments which tend to be collapsible and were found out in the entire ground of the interesting area up to a maximum depth of about 6 m b.g.l. They consist of clay of low plasticity, of hard to stiff consistency, and occasionally of loam of low plasticity, of hard to stiff consistency.

The 2<sup>nd</sup> loess horizon was detected in the entire area of interest from the depth level of 3 to 6 m b.g.l. to the depth of 9 to 11 m b.g.l. They consist of aeolian sediments represented by clay of low plasticity, of hard and stiff consistency and by loam of low plasticity, of hard and sporadically of stiff consistency.

It is necessary to point out that the aeolian sediments of the 1<sup>st</sup> and 2<sup>nd</sup> loess horizon are collapsible. This property was confirmed by the results of laboratory tests carried out on undisturbed soil samples and indirectly by the low bulk density and high

porosity of the loess(loam)s. The loess texture was even disturbed by higher load, i.e. they have collapsed without additional wetting.

Under the loessoid sediments, and over the gravel layer complex, at the depth level of about 9 to 10 m b.g.l. through 13 to 18 m b.g.l. were found degraded loesses consisting mainly of clay of low and intermediate plasticity, of hard and stiff consistency and sporadically of loam of low plasticity, of hard and stiff consistency. Typical for this horizon is the occurrence of  $\text{CaCO}_3$  nodules and strongly calcareous intercalations, the amount of which increases with depth.

Under the loess(loam) complex up to a depth of about 20 m to 22 m b.g.l. occur the alluvial sediments in the form of sand, gravel and sand-gravel mixture (layer complex C) with lime concretions up to 80 mm. In the upper part the alluvial sediments consist of fine sandy soils which pass continuously to the beneath positioned clayey-sandy and sporadically fine-grained sands. In the lower part prevails sandy, well-graded and dense to very dense gravel of high bearing capacity. In some parts of the site at the interface to the underlying gravel sandstone with a thickness of about 0.3 m has been found. From the geotechnical point of view the alluvial gravels are capable to transfer safely and without increased deformations the several times higher loads compared to the above fine soils.

The underlying stratum made up of tertiary (neogene) clays, silts and sands (layer complex D) was found up to the investigated depth of 35 m b.g.l. The tertiary sediments are composed of (clayey-)silty sand, sandy-clayey silt and clay. The plasticity of the cohesive sediments varies from medium (silts) to high and the plastic state from semi-solid to stiff (hard).

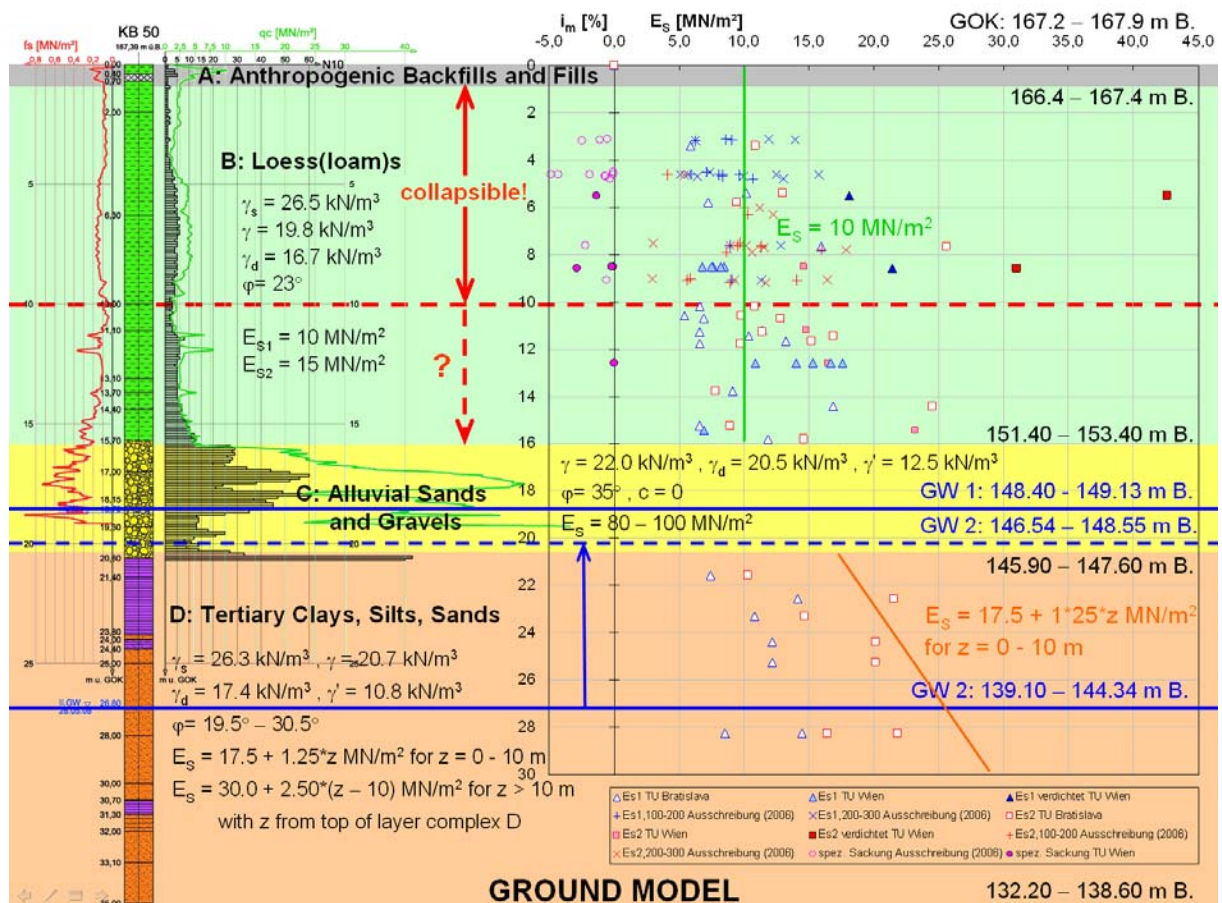


**Figure 15.** Ground model with calculation parameters for each layer.

The level of the first groundwater table (unconfined groundwater) has been encountered at about 19 m b.g.l. in the quaternary sand-gravel layer. Confined groundwater has been explored between 23 m and 28 m b.g.l. in the water bearing

tertiary layers; at the end of drilling work it has welled up from 2 m to 7 m up to between 19 m and 21 m b.g.l.

It can be summarized that even if the engineering geological condition of the site area from the standpoint of the mode of deposition seems to be relatively simple, yet in geotechnical term they are complicated because of the occurrence of loesses susceptible to collapsibility!

### **2.3. Original Foundation Concept**

The original foundation concept developed for the heavyweight structures on schematic lay-outs of the planned power plant comprised the following two foundation methods:

- original foundation concept A – shallow (spread) foundations on foundation plates (rafts) and, in case of lightweight structures, on strip footing or on an individual columns (pad);
- original foundation concept B – deep foundation by transferring the entire, mainly dynamic load (action) into the bearing (load resistant) gravelly soils of the layer complex C. It was recommended to transfer the operable load of individual structures by means of wide-section piles embedded on dense or medium dense gravelly soils as the beneath neogene clays are characterized by a severalfold lower bearing capacity. Additional investigations revealed that piles had to be embedded deeply within the tertiary sediments, thus pile length of about 35 m were necessary due to negative skin friction in the collapsible loess(loam) layer complex.

### **2.4. Innovative Hybrid Ground Improvement and Deep Foundation Concept**

The foundation measures for the planned structures of the CCPP 400 MW comprise the deep dynamic compaction method in the form of deep dynamic replacement compaction of the subsoil beneath the foundations by the deep vibro replacement technique (VRT) to produce pile-like bearing elements and to improve the soil deeply during the vibration process and stabilization of the soil above the grouted stone columns and stone columns with a lime cement binder (hybrid foundation).

In dependence of the static soil pressures there are produced grouted stone columns (foundation concept I) and stone columns (foundation concept II).

Foundation concept I which combines the deep vibro replacement technique (VRT) to produce pile-similar bearing elements (grouted stone columns, VSS) with soil stabilization beneath the foundations is carried out for the heavyweight structures. The area to be improved by the VSS-elements exceeds the foundations by about 2 m on each side. The area of the grid is defined in dependence of the static soil pressure within the following range:

- min. 1.4 m x 1.4 m = 1.96 m<sup>2</sup>
- max. 2.2 m x 2.2 m = 4.84 m<sup>2</sup>

The calculative diameter of the grouted stone columns (minimum diameter) is defined with 0.60 m. The thickness of the stabilized soil package varies between about 2 and 3 m.

Foundation concept II which combines the deep vibro replacement technique (VRT) to produce stone columns (SS) with soil stabilization beneath the foundations is carried out for lightweight structures. The area to be improved by the SS-elements exceeds the foundations by about 2 m on each side. The area of the grid is defined in dependence of the static soil pressure within the following range:

- min. 1.4 m x 1.4 m = 1.96 m<sup>2</sup>
- max. 2.5 m x 2.5 m = 6.25 m<sup>2</sup>

The calculative diameter of the stone columns (minimum diameter) is defined with 0.60 m. The thickness of the stabilized soil package is about 2 m.

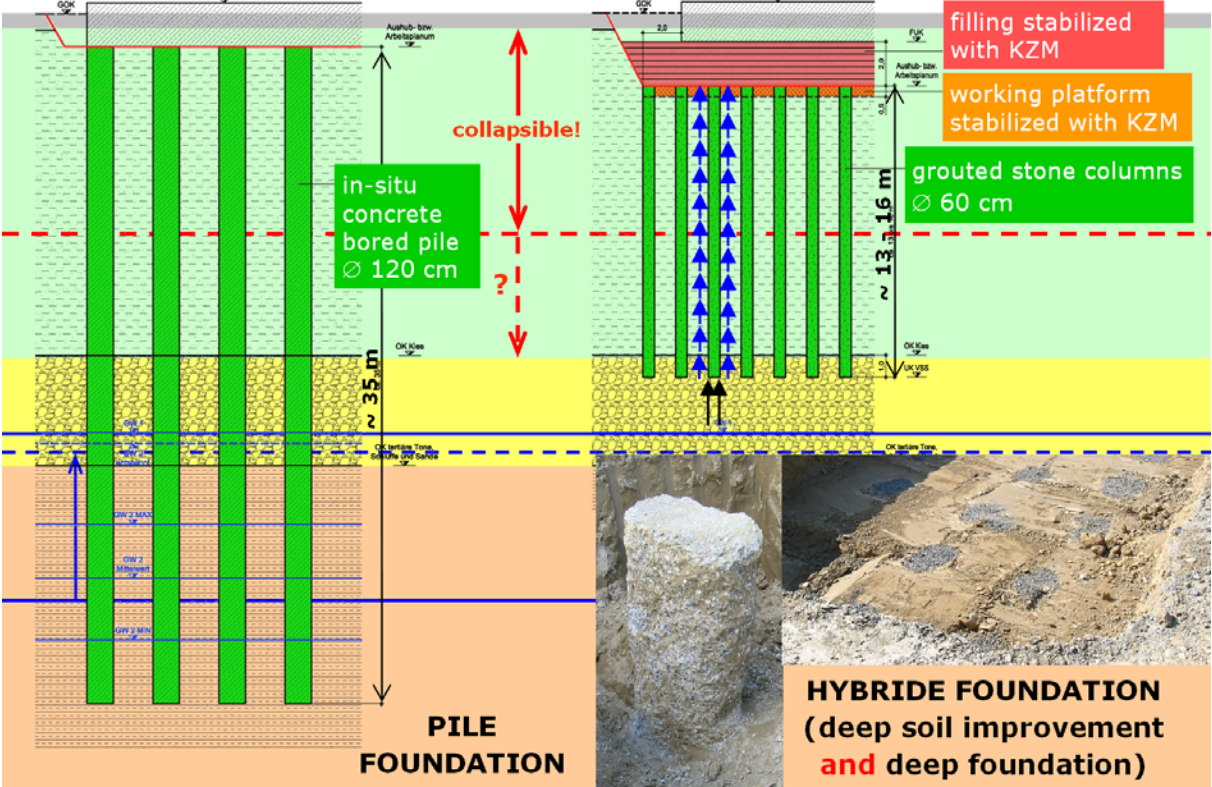


Figure 16. Original foundation concept (left) vs. hybrid foundation concept (right).

Deep vibro replacement was carried out from a working platform that is situated between 2 and 3 m below the bottom of the base slab of the single structures. After the excavation of the soil up to the required depth, the excavation level was stabilized with a lime-cement binder up to a depth of about 0.5 m. Afterwards the points for the deep vibro replacement process were pre-drilled up to the surface of the quaternary gravel using a continuous flight auger. In the pre-drilled replacement points the grouted stone columns (VSS) or stone columns (SS) were produced using the deep vibro replacement technique: The gravel was dry fed into the ground and, in the case of grouted stone columns, during the same process mixed in-situ with cement grout. Thus, a solid column was created once the grout has set. The production process allows a high flexibility and compactable loess around the column is improved by the horizontally effective dynamically excited air fed bottle-like vibrator. Consequently, beside the production of load bearing stone columns the soil is homogenized by the vibration process.

2.4.1. Soil stabilization

On the one hand the working platform for the deep vibro replacement method and on the other hand the filling up to the foundation level has been stabilized with a lime-cement mixture (KZM) using the mixed-in-place method.

*Stabilization of the working platform and foundation level*

The excavation was executed up to the required depth according to the excavation plan. The excavation level was stabilized with a lime-cement binder (KZM) according

to the Geotechnical Report up to a depth of about 0.5 m below the excavated level and subsequent dynamic compaction of the working platform. The amount of the KZM mixed in has been determined by a suitability test in the laboratory.

The excavation level has been stabilized by application of the roller-integrated Continuous Compaction Control (CCC) using a vibratory roller of the type HAMM 3414HT. The stabilized formation level was checked by dynamic load plate tests using the Light Falling Weight Device (LFWD).

If the stabilized excavation level (working platform) beneath the individual structures has met the requirements according to the Geotechnical Report, i.e. a dynamic deformation modulus of  $E_{vd} = 50 \text{ MN/m}^2$  has been proved with the Light Falling Weight Device (LFWD) about 3 days after stabilization and compaction, it has been approved for the subsequent foundation works, i.e. the deep vibro replacement works to produce (grouted) stone columns.

### *Stabilization of the filling up to the foundation level*

The filling from the level of the working platform up to the formation level of the blinding layer has been carried out in layers using the excavated loess (loam) of layer complex B and stabilizing it with a lime-cement binder (KZM) by the mixed-in-place method. After mixing in the required amount of KZM due to suitability test each layer has been compacted dynamically by application of the roller-integrated Continuous Compaction Control (CCC) using a vibratory roller of the type HAMM 3414HT.

The compaction control of each layer has been performed with dynamic load plate tests using the Light Falling Weight Device (LFWD).

Eventually each stabilized and compacted layer has met the requirements according to the Geotechnical Report, i.e. a dynamic deformation modulus of  $E_{vd} = 75 \text{ MN/m}^2$  has been proved with the Light Falling Weight Device (LFWD) about 3 days after stabilization and compaction.



**Figure 17.** Deep vibro replacement works.





**Figure 19.** Pre-drilled replacement point of the (grouted) stone columns (left foto) and excavated test column (right foto).

The improvement of the soil around the columns due to the vibration process (anticipation of collapse in the soil structure and compaction) combined with the grouted column material (deep foundation elements) characterizes the hybrid foundation concept resulting in significantly shorter deep foundation elements.

## **2.5. Foundation Works and Quality Assurance**

Foundation works (deep soil improvement and deep foundation) took place from December 2008 to April 2009 and had to be performed in the period of extraordinary bad weather conditions. Nevertheless the deep foundation works could be finished within the defined time schedule. Especially for layer wise stabilization the content of the lime-cement binder determined by a suitability test had to be adapted to the actual weather conditions according to the results of the site control measures. The working platform stabilized with lime-cement by the mixed-in-place method ensured a continuous execution of the deep vibro replacement works independent of the weather conditions.

The tests, controls and documentations performed within the geotechnical supervision of the foundation works (deep vibro replacement method – grouted stone columns and stone columns – and soil stabilization) are summarized in the following.

### **2.5.1. Quality Control of the Deep Vibro Replacement Works**

The production parameters and material use during the deep vibro replacement process were recorded and documented for each column and point respectively in order to optimize and control the production process. Quality control has been accomplished by applying an on-line monitoring system recording:

- energy consumption of the vibrator,
- insertion depth of the vibrator over time,
- production time, and
- material use for each stone column.

The recorded parameters over one day were summarized in a daily report. The documentation records of the deep vibro replacement works are collected on site.

The diameter of the grouted stone columns of 60 cm assumed for the design of the soil improvement measures and the chosen production parameters have been verified by producing a test column outside the base slab of the planned structure. After hardening the column has been excavated (see Figure 19) and cylindrical specimens have been drilled out from the column in order to determine the uniaxial

compressive strength. The determined compressive strength was about 30% to 70% above the demanded design value.

Uniaxial compression tests to control continuously the production parameters for the deep vibro replacement and to verify the required characteristic value of the compressive cube strength of the material of the VSS-element in the ultimate limit state were also performed using specimens that were produced both with cement grout („suspension specimen“) and with gravel-grout compound („mortar specimen“).

A static pile loading test has been done at one test column outside the base slab in order to verify the design load of the grouted stone columns and to get the pile load – deformation relationship.

Vibration measurements have been performed during the production of selected grouted stone columns in order to determine the attenuation of the vibrations caused by the deep vibro compaction process.

## 2.5.2. Quality Control of the Soil Stabilization Works

The suitability test of the stabilization of the working platform was carried out in-situ at a test field on the basis of dynamic load plate tests using the Light Falling Weight Device (LFWD). The content of the lime-cement binder for the layers of the filling up to the level of the blinding layer was determined on the basis of laboratory tests (suitability test in the laboratory).

The dynamic compaction of the stabilized working platform and layers of the filling up to the foundation level was carried out by application of the roller-integrated Continuous Compaction Control (CCC) using a vibratory roller of the type HAMM 3414HT.

The compaction control of each layer has been performed by with dynamic load plate tests using the Light Falling Weight Device (LFWD).

## **3. SAVA RIVER BRIDGE BELGRADE (SERBIA) DEEP FOUNDATION CONCEPT**

### **3.1. Introduction**

Sava Bridge is a 7 span, continuous superstructure with an overall length of 964 m between deck expansion joints (see Figure 20). The main support system is a single pylon asymmetric cable stayed structure with a main span of 376 m and a back span of 200 m. Four spans of 69 m, 108 m, 81 m and 81 m continue the cable stayed section and the end span connecting up the back span is of 50 m length. The pylon is 200 m high. All supports are based on pile foundations. The overall deck width is 45.04 m and shall carry 6 lanes of vehicular traffic, 2 tracks of a new light rail system and 2 lanes of a pedestrian/cycle way.

The conceptual design for the bridge was prepared by Pointing Maribor, DDC Ljubljana and CPV Novi Sad. This concept had to be respected in detailed design to be performed by the contractor (Steinkühler et al., 2010).

In 2007 the company Porr Technobau und Umwelt AG, Vienna, has been assigned for the construction of the bridge over the Sava River and entrusted both the geotechnical and the structural foundation design to the Foundation Design Consortium, consisting of three Austrian consulting engineers Geotechnik Adam ZT GmbH, Stella and Stengl & Partner, and IBBS Schweighofer. Geotechnical

investigation works were done by the Faculty of Mining and Geology of Belgrade University, Serbia, additional soil laboratory tests were performed at the Institute for Geotechnics at Vienna University of Technology, Austria.

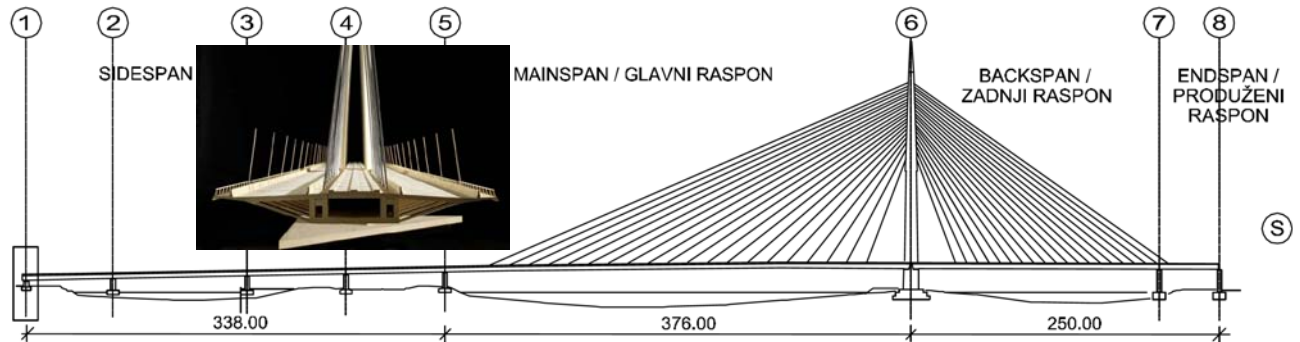


**Figure 20.** Layout of the new bridge over the Sava River and cross section of the bridge deck.

### 3.2. Ground conditions

Referring to reports on interpretation of soil investigations the following geological profile of the ground was derived from 7 boreholes in the conceptual design phase and 13 additional boreholes for detailed design (see Figure 21) (Hinterplattner et al., 2011):

- Layer n : Embankment as artificial surface cover
- Quaternary sediments:
  - o Layer G-al: Silty sandy clays with mud interbeds and lenses – facies of flood plain
  - o Layer P-al: Medium-grained to fine-grained sands – river bed facies
  - o Layer S-al: Gravels – river (fluvial) lacustrine sediments
- Tertiary sediments:
  - o Layer M: Weathered marly clays and marls and below grey unaltered marls (not registered in boreholes around Piers No. 7 and 8)
  - o Layer R: Limestone, sandstones
- Basic geological substratum:
  - o Cretaceous sediments

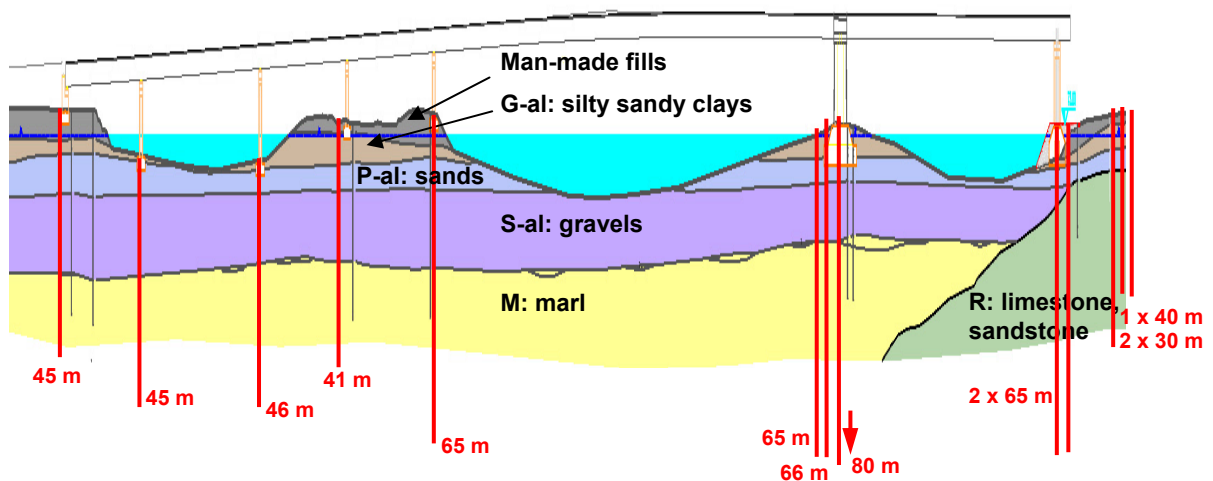


**Figure 21.** Geological longitudinal section (not to scale) and situation of additional exploration borings (red).

Ground water is strongly influenced by the water level of the Sava River. E.g. at Pier 6 ground water level is 1.48 m above surface in case of high navigation level (HNL) and subsoil is saturated. In case of low navigation level (LNL) the ground water level is in a depth of 2.18 m. In the ground 4 hydro-geological complexes were defined.

Piles for all pier foundations were embedded into the low deformable tertiary sediments in order to reduce settlements significantly. Grey unaltered marls have exactly the same textural characteristics as the elevated (roof) weathered marly clays and marls. Their thickness is from 20 to over 30 m. They are characterized by extremely massive texture. Lithological banding is manifested by colour. The increased carbonate content gives the rock a greyish white colour in contrast to the parts with smaller carbonate content, which are grey. Inclination of lithological banding (bedding) surface amounts to around 3° to 5°. The lithological banding surfaces, especially when they are encountered in the form of thin “film” of sandy mass, represent latent mechanical discontinuities. They are over-consolidated and hard with conchoidal rupture. The marls are poorly compressible and are practically impermeable. In relation to physical-mechanical properties, in mm to cm observation area, they represent poorly heterogeneous and anisotropic environment, whereas in the larger metric observation area they are practically homogenous and isotropic. These tertiary sediments were not explored in boreholes in the area of Piers 7 and 8 (see Figure 22).

Limestone is of Sarmatian age and is represented by sandy phytogenous detritus full of fauna, in places with fossilized mollusc lumachelle. Because of carstification, this phytogenous rarely sandy limestone (calcarenite) is riddled with caverns and fractures of various sizes and in the near-surface area, mostly filled with material from the elevated (roof) stratum. Their structure is massive and in certain parts brecciate. Thicknesses vary from several meters to several tens of meters. They are usually encountered under grey marls. Their contact with underlying Cretaceous sediments is discordant.

Cretaceous sediments represent the basic geological substratum of the ground. Most of flysch is composed of sandstones, which alternates with siltstones and clayey shale. Micro conglomerates are rarely encountered.

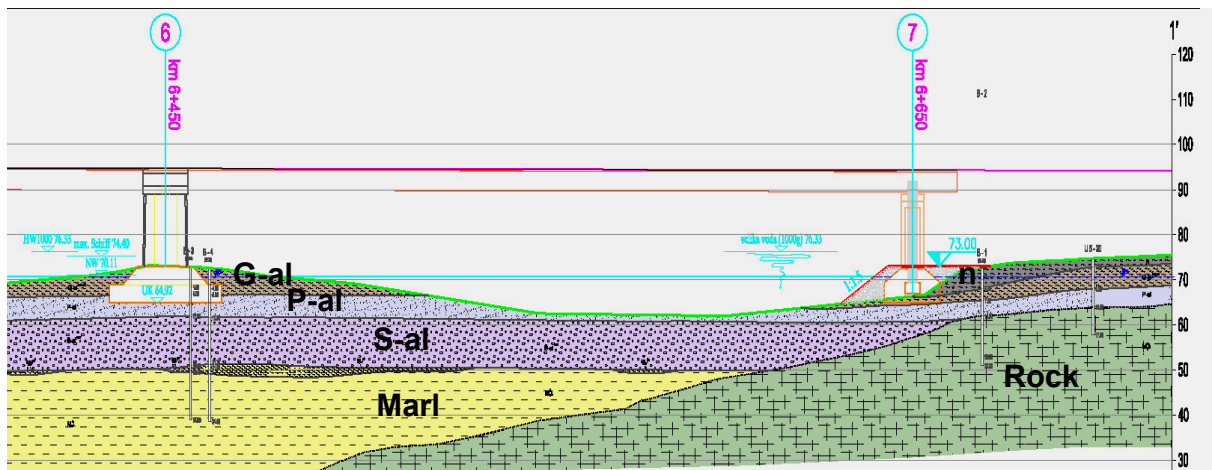


**Figure 22.** Layout of the new bridge over the Sava River and cross section of the bridge deck.

### 3.3. Soil parameters

Based on the performed ground explorations and soil investigations calculation parameters for geotechnical design were derived in particular from laboratory tests performed in the conceptual design phase and in the detailed design phase at

Belgrade University and Vienna University of Technology. The particular laboratory tests have been concluded in tables and analysed statistically (Geotechnik Adam ZT GmbH, 2009). The following characteristic soil parameters were derived from statistical evaluation, empirical data and cautious selection with engineering judgment.

**Table 3:** Characteristics soil parameters for geotechnical design (Geotechnik Adam ZT GmbH, 2009).

layer	description (unified classification (USCS))	weight density	effective weight density	saturated weight density	effective shear angle	cohesion	oedometer modulus	deformation modulus
		$\gamma$	$\gamma'$	$\gamma_{sat}$	$\phi'$	$c$	$E_{oed}$	$E_d$
		[kN/m <sup>3</sup> ]	[kN/m <sup>3</sup> ]	[kN/m <sup>3</sup> ]	[°]	[kN/m <sup>2</sup> ]	[MN/m <sup>2</sup> ]	[MN/m <sup>2</sup> ]
<b>n</b>	Embankment	19.5	10.0	20.0	25	0	n.r.	n.r.
<b>G-al</b>	Silty-sandy clays with mud interbeds and lenses (CL, CH, MH)	18.5	8.5	18.5	25	0	2	n.r.
<b>P-al</b>	Medium-grained to fine-grained sands – river bed facies (SU)	18.5	9.0	19.0	30	0	10	n.r.
<b>S-al</b>	Gravels – River (fluvial)-lacustrine sediments (GP)	22.5	12.5	22.5	35	0	30	n.r.
<b>M- lg,l*</b>	Weathered marly clays and marls	18.0	8.5	18.5	25	0	25	n.r.
<b>M-L</b>	Grey unaltered marls	18.5	9.0	19.0	30	20	60 - 100	n.r.
<b>M-K</b>	Limestone (rock monolith)	22.0	n.r.	n.r.	n.r.	n.r.	n.r.	≥ 2000
<b>M-ps</b>	Sandstone (rock monolith)	25.0	n.r.	n.r.	n.r.	n.r.	n.r.	≥ 8000
<b>K</b>	Cretaceous sediments	n.r.	n.r.	n.r.	n.r.	n.r.	n.r.	n.r.

**Table 4:** Characteristic soil parameters for derivation of shaft friction and base resistance pressure according to technical provisions (Geotechnik Adam ZT GmbH, 2009).

layer	description	undrained shear strength	cone penetration resistance (CPT)	uniaxial compression strength	number of blows (SPT)
		$c_u$	$q_c$	$q_u$	$N$
		[kN/m <sup>2</sup> ]	[MN/m <sup>2</sup> ]	[kN/m <sup>2</sup> ]	[-]
<b>n</b>	Embankment	-	1	-	3
<b>G-al</b>	Silty-sandy clays with mud interbeds and lenses	-	1	-	3
<b>P-al</b>	Medium-grained to fine-grained sands - river bed facies	-	5	-	15
<b>S-al</b>	Gravels – River (fluvial)-lacustrine sediments	-	15	-	45
<b>M- lg,l*</b>	Weathered marly clays and marls	200	3	400	-
<b>M-L</b>	Grey unaltered marls	900	11	1800	-

**Table 4:** Characteristic soil parameters for derivation of shaft friction and base resistance pressure according to technical provisions (Geotechnik Adam ZT GmbH, 2009).

layer	description	undrained shear strength	cone penetration resistance (CPT)	uniaxial compression strength	number of blows (SPT)
		$c_u$ [kN/m <sup>2</sup> ]	$q_c$ [MN/m <sup>2</sup> ]	$q_u$ [kN/m <sup>2</sup> ]	N [-]
M-K	Limestone (rock monolith)	-	-	≥ 1000	-
M-ps	Sandstone (rock monolith)	-	-	≥ 5000	-
K	Cretaceous sediments	-	-	-	-

### 3.4. Deep Foundation Design Concept

#### 3.4.1. Design concept for pile group foundations of Piers 1 to 5 and Piers 7 and 8

Pile group foundations at Piers 1 to 5 as well as Piers 7 and 8 are composed of single piles with a defined spacing between the piles forming pile groups. The bearing capacity of a single pile consists of the total shaft resistance (derived from shaft friction) and the activated base resistance force (derived from base resistance). Overall bearing capacity of a pile group foundation depends on the pile spacing as well and therefore has to be taken into account. Pile spacing has to be  $e \geq 2.5 D$  otherwise a reduction of shear parameters is necessary.

**Table 5:** Partial safety factors and correlation factors to evaluate the results of static pile load tests according to ÖNORM B 1997-1-1 (2007) (this code with national specifications and national supplements is not available in English language; translated by the author).

*Table 5: Partial safety factors on the effects of actions ( $\gamma_E$ )*

action		symbol	value		
duration	condition		BS 1	BS 2	BS 3
permanent	unfavourable	$\gamma_G$	1.35	1.20	1.00
	favourable	$\gamma_G$	1.00	1.00	1.00
variable	unfavourable	$\gamma_Q$	1.50	1.30	1.00
	favourable	$\gamma_Q$	0	0	0

*Table 6: Partial safety factors for soil parameters ( $\gamma_M$ )*

soil parameter	symbol	value
angle of shearing resistance <sup>a</sup>	$\gamma_{\varphi'}$	1.00
effective cohesion	$\gamma_{c'}$	1.00
undrained shear strength	$\gamma_{c_u}$	1.00
unconfined strength	$\gamma_{q_u}$	1.00
weight density	$\gamma_\gamma$	1.00

<sup>a</sup>) this factor is applied to  $\tan \varphi'$

*Table 7: Partial resistance factors ( $\gamma_R$ ) for driven piles, bored piles and continuous flight auger piles*

resistance	symbol	value
base	$\gamma_b$	1.10
shaft (compression)	$\gamma_s$	1.10
total/combined (compression)	$\gamma_t$	1.10
shaft in tension	$\gamma_{s:t}$	1.15

*Table 8: correlation factors ( $\xi$ ) to derive characteristic values from static pile load tests*

$\xi$ for n =	1	2	3	4	$\geq 5$
$\xi_1$	1.40	1.30	1.20	1.10	1.00
$\xi_2$	1.40	1.20	1.05	1.00	1.00
<b>n number of tested piles</b>					

Verification of vertical bearing capacity was performed according to EN 1997-1 (EC7, 2006). The partial safety factors were assessed according to the national specifications concerning ÖNORM EN 1997-1 (2006) and national supplements. Table 5 contains the partial safety factors and correlation factors to evaluate the results of static pile load tests according to ÖNORM B 1997-1-1 (2007) for the design of the pile foundations.

In the scope of the objective project no tension piles were expected so that an overall valid partial safety factor was assessed according to ÖNORM B 1997-1-1, Table 7 (2007):

$$\gamma_R = 1.10.$$

At Piers 5, 6, and 7 pile load tests were carried out. By means of the comparable stratigraphy of the ground at Piers 1 to 6 the results of pile load tests at Piers 5 and 6 could be transferred to Piers 1 to 4 as well. Consequently, the following spreading factors were selected according to ÖNORM B 1997-1-1 Table 8:

$$\begin{aligned} \xi_1 &= 1.40 \quad (n = 1) \\ \xi_2 &= 1.40 \quad (n = 1) \end{aligned}$$

### 3.4.2. Design concept for the box-shaped foundation of the pylon at Pier 6

Box-shaped foundation beneath pylon at Pier 6 is composed of a compound body consisting of an encasing diaphragm wall and piles as well as the enclosed soil. This quasi-monolith transfers high vertical and horizontal forces. Piles and capping raft form a box, which acts physically like a “pot” turned upside down. Consequently, the settlements are smaller than for conventional pile groups, and the earthquake resistance is significantly higher. Box-shaped foundations represent a special form of piled raft foundations utilising the enclosed soil core as an integrated load transfer member.

The following two calculation models were applied. They have proved satisfactory in the design of several bridges over the river Danube in Austria (Fross et al., 2010).

### *Calculation model A: Single piles and diaphragm wall*

- Evaluating the bearing capacity of single elements they provide only fictitious limit case values because the bond effect between concrete elements and enclosed soil core is neglected. Thus, maximum pile or diaphragm wall loads are calculated.
- Verification of vertical bearing capacity is performed according to EN 1997-1 (EC 7).
- Shaft friction is taken into account at outer and inner box surfaces (including the pile rows) and base resistance forces of the single piles and the diaphragm wall.

### *Calculation model B: Quasi-monolithic*

- According to Brandl (2003) a full bond effect between deep foundation elements and the closed soil is assumed. This compound body comprises the outer circumference of the foundation if secant piles or diaphragm walls are installed. In the case of contiguous piles the theoretical area should be reduced by at least half a pile diameter. For the quasi-monolith, only shaft friction along the outside surface of the foundation box may be taken into account.
- The monolith-theory provides minimum pile or diaphragm wall loads. However, a full composite effect occurs only theoretically but hardly in practice. Therefore, relatively high safety factors are required. According to Brandl (2003) calculations should be based on a global safety factor of  $\eta \geq 3.0$ , if conventional calculation methods for evaluating the base failure of equivalent "shallow" foundations are used.
- According to Brandl (2003) a global safety factor of ground failure of the raft foundation for river bridge foundations of  $\eta = 3.5$  is used.
- Shaft friction is effective only around the outer perimeter of the box-shaped foundation.
- The base pressure is assumed to be effective over the entire base area of the monolith. The base pressure should not exceed the actual overburden stress multiplied by the over consolidation ratio (OCR) of the marl in order to minimize foundation settlements and differential settlements. OCR was determined with particular tests in the scope of laboratory investigations. Taking into account an average weight of soil of 20 kN/m<sup>2</sup> OCR ranges from 950 to 1,940 kN/m<sup>2</sup> at bridge site.

### *For seismic foundation design two approaches were considered:*

On the one hand dynamic soil parameters can be determined from geophysical field tests (e.g. cross-hole and down-hole tests) and/or dynamic laboratory tests (e.g. resonant columns test). Field tests deliver elastic data (dynamic shear modulus and dynamic elastic modulus) at small shear strains. However, increasing shear strains produce a reduction of the dynamic stiffness parameters. Depending on the seismic load and the corresponding shear strain the dynamic parameters can be identified. Stiffness matrix and damping matrix can be determined by using a suitable model, whereby radiation damping is represented by the damping matrix. However, radiation damping is always beneficial for the structure, thus neglecting this effect gives a solution on the safe side.

On the other hand seismic calculations can be performed by variation of the static stiffness, if radiation damping can be neglected. In general, the quasi-static stiffness increases when dynamic loads are applied. In the scope of the seismic design of the foundations of the Sava Bridge parametric studies were performed taking into account both approaches. Dynamic soil parameters were derived from geophysical tests and data given by the Serbian Seismic Institute in Belgrade. A comparison of dynamic and quasi-static solutions yielded that the dynamic approach overestimated the spring stiffness by means of the assumed rigid foundation behaviour during

seismic load because the overall stiffness of the system was limited by the inherent rigidity of the foundation itself.

Thus, following parameters were chosen from the parametric studies:

- Lower limit: static value of horizontal and vertical modulus of subgrade reaction
- Upper limit: 10 times the static value of horizontal and vertical modulus of subgrade reaction

Characteristic values for shaft resistance and base resistance pressure needed not to be modified from static values. Consequently, in a case of an earthquake stiffening of the ground occurs, thus causing higher reaction forces but lower deformations. A softening of the ground can be excluded since the expected shear strains in the soil are small taking into account the magnitude of a presumed earthquake and the liquefaction potential of the layered ground is negligible (Geotechnik Adam ZT GmbH, 2009).

### 3.4.3. Geotechnical design parameters

For calculation and both static and seismic design of bored piles and diaphragm walls the following geotechnical soil parameters were specified for each pier:

- Shaft friction
- Base resistance pressure
- Horizontal subgrade reaction
- Vertical subgrade reaction

*Shaft friction and base resistance pressure:*

ÖNORM EN 1997-1 (EC 7, 2006) includes no specifications related to the definition of shaft friction and base resistance pressure. For that reason other technical provisions need to be stressed. Hitherto in Austria ÖNORM B 4440 (2001) has been used for the determination of design axial pile loads according to the global safety concept including the design base resistance pressure and the design shaft friction. In contrary the ÖNORM EN 1997-1 (EC 7, 2006) is based on the partial safety concept so that design values defined in ÖNORM B 4440 (2001) cannot be directly adopted for applications according to the partial safety concept.

ÖNORM B 1997-1-3 (draft, 2007) is currently established by the Austrian Standard Institute. The new standard will replace ÖNORM B 4440 (2001) and will cover all pile types. Amongst others procedures for determination of characteristic values for ultimate limit state (ULS) and serviceability limit state (SLS) will be defined in tables including the base resistance pressure and shaft resistance (see Tables 4, 5, 6). The design value of pile resistance  $R_{c;d}$  for a bored pile at pressure is defined by:

$$R_{c;d} = R_{c;k} / (\gamma_t \cdot \eta_{P;c})$$

with

- $\gamma_t$ : partial safety factor of pile resistance; according to ÖNORM B 1997-1-1 Table 7:  $\gamma_t = 1.10$ .
- $\eta_{P;c}$ : scale factor (model factor) for axially loaded piles at pressure; according to ÖNORM B 1997-1-3 (draft) Table A.5 resp. ÖNORM B 1997-1-1:  $\eta_{P;c} = 1.30$ .
- $R_{c;k}$ : characteristic pile resistance as a result of shaft resistance and base resistance pressure; according to ÖNORM B 1997-1-3 (draft) Table C.4 to C.7.

**Table 6:** Tables from new ÖNORM B 1997-1-3 (draft October 2007; this draft is not available in English language; translated by the author).

*Table A.5: scale factors (model factors) ( $\eta$ )*

case	symbol	value
resistances of static pile load tests (axial compression)	$\eta_{P;c}$	1.0
resistances of static pile load tests (axial tension)	$\eta_{P;t}$	1.0
resistances of the tables of annex C and D (axial compression)	$\eta_{P;c}$	1.3
resistances of the tables of annex C and D (axial tension)	$\eta_{P;t}$	2.5
box shaped foundation	$\eta_{KG}$	? *
combined raft-pile foundation	$\eta_{KPP}$	? *

*Table C.1: Coherences between SPT results in the borehole and density index of coarse grained soils and between consistency index and condition of fine grained soils*

coarse grained soil	
SPT number of blows $N_{30}$ (penetration of 30cm)	density index
0 to 4	very loose
more than 4 to 10	loose
more than 10 to 30	medium dense
more than 30 to 50	dense
more than 50	very dense
fine grained soil	
consistency index $I_c = \frac{w_l - w}{I_p}$	condition
0.0 to 0.25	pappy
more than 0.25 to 0.50	very soft
more than 0.50 to 0.75	soft
more than 0.75 to 1.00	firm
more than 1.00	semi hard

*Table C.2: Minimum embedding depth in coarse soil layers of low plasticity*

density index	SPT number of blows $N_{30}$	minimum embedding depth $l_{min}$
very dense	more than 50	d
dense	more than 30 to 50	2 d
medium dense	more than 10 to 30	3 d

*Table C.3: Minimum embedding depth in fine grained soil layers of low plasticity*

consistency	minimum embedding depth $l_{min}$
semi hard to hard	d
firm	2 d

**Table 7:** Tables from new ÖNORM B 1997-1-3 (draft October 2007; this draft is not available in English language; translated by the author).

*Table C.4: Characteristic base resistance of piles ( $q_{b;k}$ ) in coarse grained (non-cohesive) soils, depending on  $N_{30}$  -values (SPT)*

specific settlement of pile cap $s/D_b$	characteristic base resistance of piles ( $q_{b;k}$ ) in widely grained sand and sand-gravel mixtures		
	medium dense <sup>1)</sup>	dense <sup>2)</sup>	very dense <sup>3)</sup>
	MN/m <sup>2</sup>	MN/m <sup>2</sup>	MN/m <sup>2</sup>
0.005	0.30	0.40	0.50
0.01	0.55	0.80	1.00
0.02	1.05	1.40	1.75
0.03	1.35	1.80	2.25
0.05	1.90	2.50	2.95
0.075	2.50	3.10	3.55
0.10 (=s <sub>g</sub> )	3.00	3.50	4.00

<sup>1)</sup>  $N_{30}$  -value  $\geq 10$   
<sup>2)</sup>  $N_{30}$  -value  $\geq 30$   
<sup>3)</sup>  $N_{30}$  -value  $\geq 50$   
Intermediate values may be obtained by linear interpolation

*Table C.5: Characteristic base resistance of piles ( $q_{b;k}$ ) in fine grained (cohesive) soils, depending on consistency index  $I_c$*

specific settlement of pile cap $s/D_b$	Characteristic base resistance of piles ( $q_{b;k}$ ) in silt, clayey silt and clay		
	stiff <sup>1)</sup>	very stiff <sup>2)</sup>	semi solid <sup>3)</sup>
	MN/m <sup>2</sup>	MN/m <sup>2</sup>	MN/m <sup>2</sup>
0.005	0.10	0.15	0.25
0.01	0.15	0.30	0.45
0.02	0.35	0.60	0.90
0.03	0.45	0.80	1.15
0.05	0.60	1.10	1.60
0.075	0.70	1.40	2.00
0.10 (s = s <sub>g</sub> )	0.80	1.50	2.20

<sup>1)</sup>  $I_c \geq 0.75$   
<sup>2)</sup>  $I_c \geq 0.90$   
<sup>3)</sup>  $I_c > 1.00$   
Intermediate values may be obtained by linear interpolation

**Table 8:** Tables from new ÖNORM B 1997-1-3 (draft October 2007; this draft is not available in English language; translated by the author).

*Table C.7: Characteristic shaft resistance of piles ( $q_{s;k}$ ) in fine grained (cohesive) soils, depending on consistency index  $I_c$  respectively on unconfined compressive strength  $q_u$*

specific settlement of pile cap $s/D_b$	Characteristic base resistance of piles ( $q_{b;k}$ ) in silt, clayey silt and clay		
	stiff <sup>1)</sup>	very stiff <sup>2)</sup>	semi solid <sup>3)</sup>
	MN/m <sup>2</sup>	MN/m <sup>2</sup>	MN/m <sup>2</sup>
0.005	0.10	0.15	0.25
0.01	0.15	0.30	0.45
0.02	0.35	0.60	0.90
0.03	0.45	0.80	1.15
0.05	0.60	1.10	1.60
0.075	0.70	1.40	2.00
0.10 ( $s = s_g$ )	0.80	1.50	2.20

<sup>1)</sup>  $I_c \geq 0.75$   
<sup>2)</sup>  $I_c \geq 0.90$   
<sup>3)</sup>  $I_c > 1.00$   
Intermediate values may be obtained by linear interpolation

*Table C.6: Characteristic shaft resistance of piles ( $q_{s;k}$ ) in coarse grained (non-cohesive) soils, depending on N30-values (SPT)*

coarse grained soils		characteristic shaft resistance ( $q_{s;k}$ )	
		for serviceable limit state SLS	for ultimate limit state ULS
density index	N <sub>30</sub> -value (SPT)	MN/m <sup>2</sup>	MN/m <sup>2</sup>
loose	4	0.030	0.045
medium dense	10	0.050	0.075
	20	0.060	0.090
dense	30	0.070	0.105
	40	0.095	0.142
very dense	$\geq 50$	0.120	0.180

Intermediate values may be obtained by linear interpolation

The characteristic values for shaft resistance and base resistance pressure of piles in soil given in the following were specified on results of ground investigations and empirical values, which have already been adopted in the draft version of ÖNORM B 1997-1-3 (draft, 2007). The characteristic values for shaft resistance and base resistance pressure of piles in rock (limestone and sandstone at Pier 7) were specified according to DIN 1045 – Appendix B, Table B.5 (2005) (failure values). For geotechnical design of the pile group foundations at Piers 1 to 5 and the box-shaped foundation at Pier 6 characteristic values for shaft friction and base resistance pressure given in Table 7 were derived (Geotechnik Adam ZT GmbH, 2009).

**Table 9:** Characteristic values of shaft friction and base resistance pressure of single piles.

layer	description	shaft friction $q_{s,k}$ [kN/m <sup>2</sup> ]	base resistance pressure $q_{b,k}$ [kN/m <sup>2</sup> ]		
			s/D=0.02	s/D=0.03	s/D=0.05
P-al	Medium-grained to fine-grained sands - river bed facies	40	-	-	-
S-al	Gravels – River (fluvial)-lacustrine sediments	140	-		
M- lg,l*	Weathered marly clays and marls	60	-	-	-
M	Grey unaltered marls	80	900	1,150	1,600
M-K	Limestone	126	1,880		

The pile foot is embedded within sound marl; the vertical modulus of subgrade reaction was defined in the following range taking into account the single pile load, the stiffness modulus of the soil, and the expected settlement:

$$k_{s,v} = 75 - 83 \text{ MN/m}^3$$

For the design of the pile foundation the distribution of the horizontal modulus of subgrade reaction presented in Table 10 was applied, which was determined from SPT, CPT, and further ground investigation (Geotechnik Adam ZT GmbH, 2009).

**Table 10:** Horizontal modulus of subgrade reaction.

depth	modulus of horizontal subgrade reaction	distribution of modulus of horizontal subgrade reaction
above top of layer P-al	0 MN/m <sup>3</sup>	linear
bottom of layer P-al	25 MN/m <sup>3</sup>	
top of layer S-al	50 MN/m <sup>3</sup>	linear
bottom of layer S-al	100 MN/m <sup>3</sup>	
top of weathered marl M- lg,l*	100 MN/m <sup>3</sup>	constant
bottom of weathered marl M- lg,l*	100 MN/m <sup>3</sup>	
below top of grey unaltered marls M	150 MN/m <sup>3</sup>	constant

At Piers 7 and 8 the rock surface was found in a depth of about 17 m below actual ground surface, thus tip resistance piles (end bearing piles) had to be carried out. For geotechnical design of the pile foundation (pile group) characteristic values for shaft friction and base resistance pressure (see Table 11) were applied (Geotechnik Adam ZT GmbH, 2009).

**Table 11:** Characteristic values of shaft friction and base resistance pressure of single piles. Rock values according to DIN 1054 (2005).

layer	description	shaft friction $q_{s,k}$ [kN/m <sup>2</sup> ]	base resistance pressure $q_{b,k}$ [kN/m <sup>2</sup> ]		
			s/D=0.02	s/D=0.03	s/D=0.1
G-al	Silty-sandy clays with mud interbeds and lenses	0	-	-	-
P-al	Medium-grained to fine-grained	0	-	-	-

**Table 11:** Characteristic values of shaft friction and base resistance pressure of single piles. Rock values according to DIN 1054 (2005).

layer	description	shaft friction $q_{s,k}$ [kN/m <sup>2</sup> ]	base resistance pressure $q_{b,k}$ [kN/m <sup>2</sup> ]		
			s/D=0.02	s/D=0.03	s/D=0.1
	sands - river bed facies				
<b>S-al</b>	Gravels – River (fluvial)-lacustrine sediments	0	-		
<b>M-K</b>	Limestone	126	-		
<b>M-ps</b>	Sandstone	500	5,000		

If the pile foot is embedded within the sound rock, the vertical modulus of subgrade reaction is defined in the following range taking into account the single pile load, the stiffness modulus of the soil, and the expected settlement:

$$k_{s,v} = 1,000 \text{ MN/m}^3$$

For the design of the pile foundation the distribution of the horizontal modulus of subgrade reaction presented in Table 12 was applied, which has been determined from SPT, CPT, and further ground investigation (Geotechnik Adam ZT GmbH, 2009).

**Table 12:** Horizontal modulus of subgrade reaction.

depth	modulus of horizontal subgrade reaction	distribution of modulus of horizontal subgrade reaction
above top of layer M-K	0 MN/m <sup>3</sup>	-
top of laver M-K	100 MN/m <sup>3</sup>	linear
bottom of laver M-K	200 MN/m <sup>3</sup>	
below top of laver M-ps	500 MN/m <sup>3</sup>	constant

Following additional specifications had to be considered:

- Overall bearing capacity of a pile group foundation depends on the pile spacing as well and therefore has to be taken into account. Pile spacing has to be  $e \geq 2.5 \cdot D$ , otherwise a reduction of shear parameters has to be performed.
- Distance of excavation level to bedding zone has to be  $\geq 3.0$  m.
- Horizontal stresses in the bedding zone must not exceed the passive earth pressure.
- Group factors  $\alpha_L$  and  $\alpha_Q$  according to DIN 1054 have to be considered.
- According to DIN 1054 (2005) and ÖNORM B 1997-1-3 (draft, 2007) a minimum embedding depth in the sound marl of  $t_E \geq 5$  m has to be taken into account.

In Figure 23 the geotechnical design parameters derived from the soil parameters taking into account the applied standards according to EC 7 (2006) are illustrated for Pier 6 (box-shaped foundation embedded in marl) and Pier 7 (pile group foundation embedded in rock).

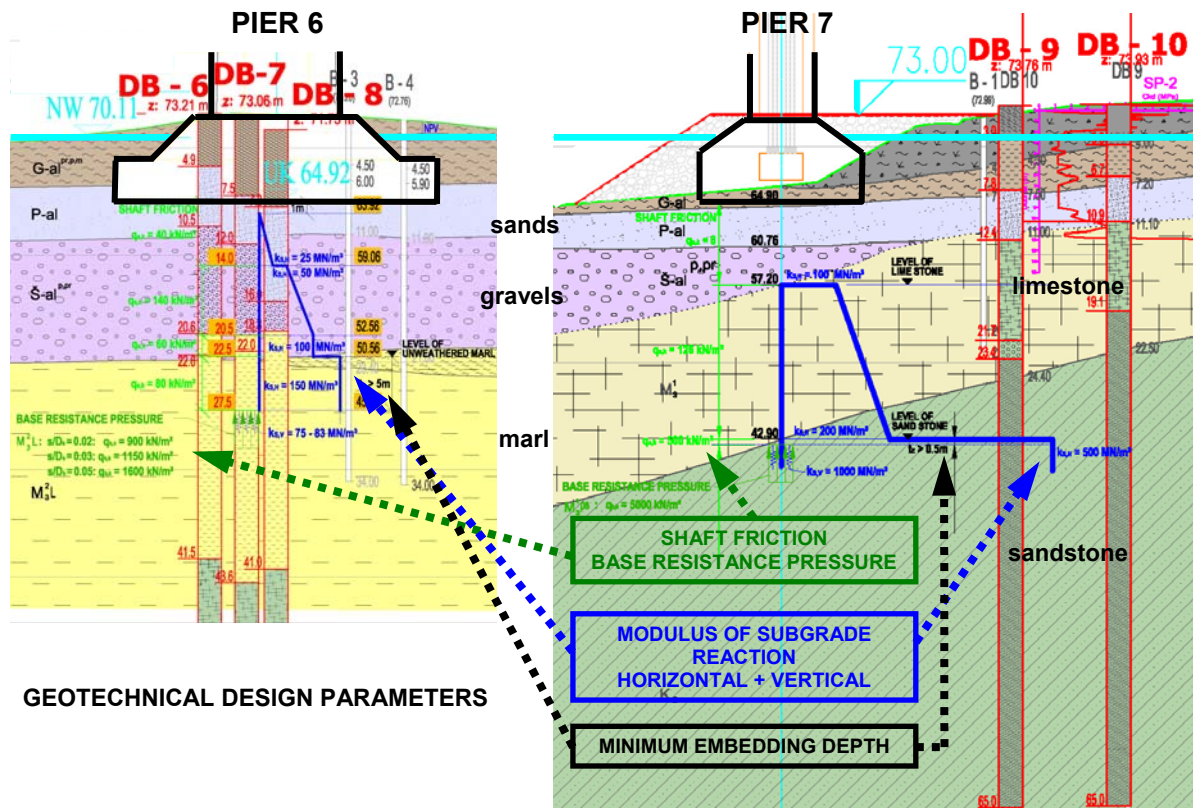


**Figure 23.** Geotechnical design parameters exemplary for Pier 6 (left) and Pier 7 (right).

### 3.5. Box-shaped Foundation for the Pylon at Pier 6

#### 3.5.1. Layout and calculation model for box-shaped foundation

In the following the box-shaped foundation for the pylon at Pier 6 is described in more detail. It consists of an encasing diaphragm wall and piles inside (see Figure 24):

- Piles: 113 piles with a diameter of 1.5 m
- Pile length: 29.0 m
- Diaphragm wall: thickness of 1.0m, length of 37 m
- Pile cap: diameter of 25.0, 30.0 and 34.0 m and a total thickness of 8.0 m

The total load (serviceability limit state) amounts to 602 MN, whereas dead load of piles, diaphragm wall and pile cap are not included. The maximum working load of a single pile is 3.7 MN. Taking into account the additional load due to the dead load of the pile raft (uplift is considered for ground water level at low navigation level), the maximum working load of a single pile amounts to 4.4 MN (Hinterplattner et al, 2011).

Compared to the original conceptual design a reduction of the number of piles could be achieved. The encasing diaphragm wall served as retaining wall for the construction pit of the pile raft as well. Thus, no additional measures were necessary to secure the construction pit against earth pressure, traffic loads and water pressure in particular in case of floods.

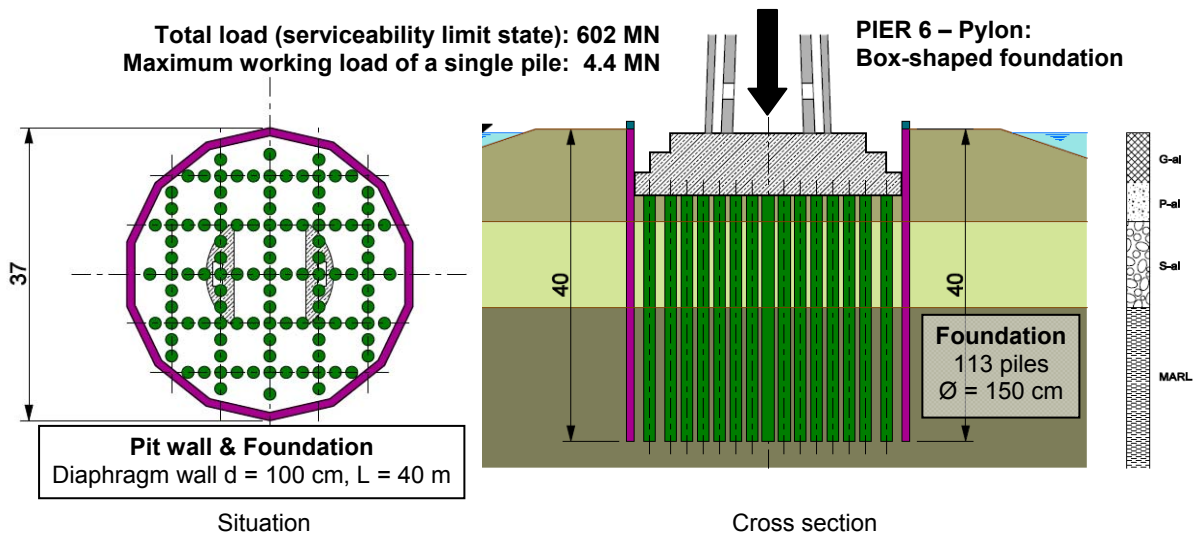


**Figure 24.** Layout of the box-shaped foundation for the pylon at Pier 6.

The calculation model for the foundation substructure illustrated in Figure 25 was established considering the geometry and the stiffness of the foundation elements (diaphragm wall, piles, and pile raft). The ground reaction was derived from the horizontal and the vertical modulus of subgrade reaction to be effective at the base and the vertical diaphragm panels. The stress resultant components ( $V_z$ ,  $H_x$ ,  $H_y$ ,  $M_x$ ,  $M_y$ ,  $M_T$ ) and both the displacement ( $u_x$ ,  $u_y$ ,  $u_z$ ) and the rotation/torsion components ( $\psi_{x_x}$ ,  $\psi_{y_y}$ ,  $\theta_z$ ) (in total resulting in 6 degrees of freedom) were calculated for a unit load at the top centre of the pile raft in order to derive the stiffness matrix of the box-shaped foundation compound interacting with the bridge superstructure. Stresses and deformations were then determined applying the substructure technique coupling the foundations of all piers with the bridge superstructure.

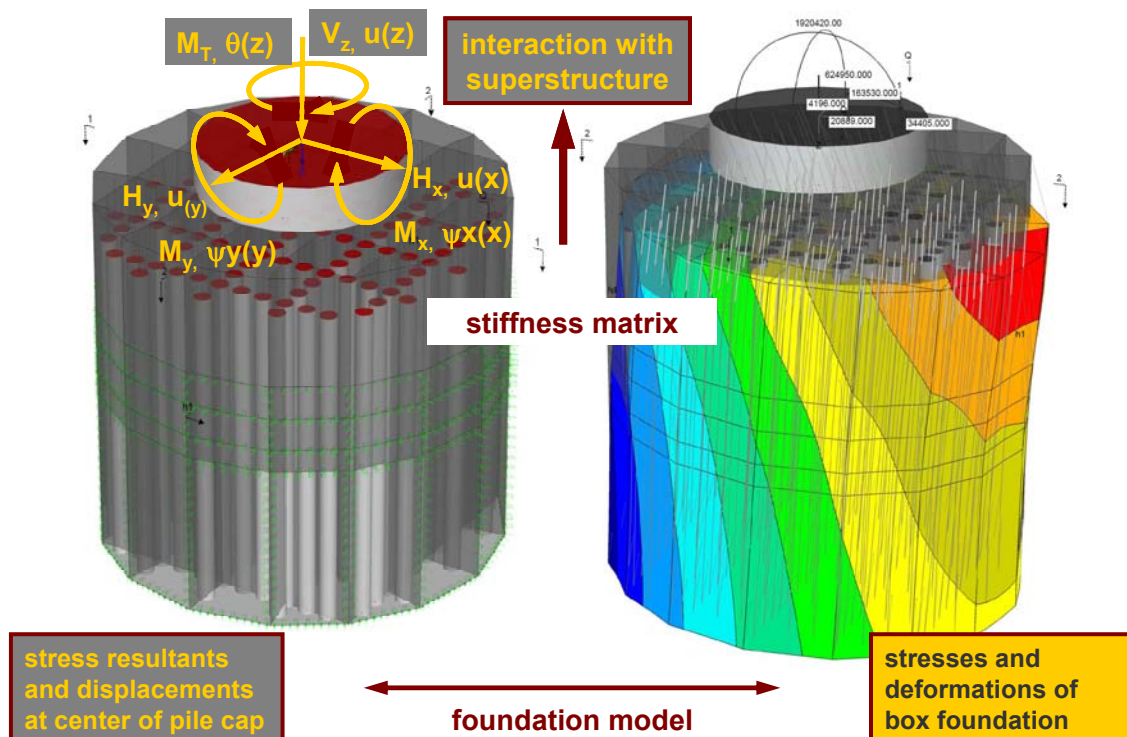


**Figure 25.** Calculation model for boxed-shaped foundation of pylon at Pier 6 and stiffness matrix.

### 3.5.2. Trial piles

In order to verify soil parameters used for calculation and design of pile foundations of Sava-Bridge four trial piles at Piers 5, 6 and 7 were installed and tested. The test load was assessed as the working load multiplied by a safety factor of 2.125 according to EC 7-1 (design situation BS1).

As an example Figure 26 shows measurement results of trial pile No. 2, situated at Pier 6, with a diameter of 1.5 m, a length of 38.1 m and a maximum test load of 9.6 MN (considering a working load of 4.4 MN). Up to a depth of 8 m, which corresponds to a depth of designed pile raft, an elimination pipe was installed in order to avoid skin friction within the upper soil layers. At the maximum load stage measured settlements were 7.3 mm, with a plastic portion of 2.7 mm. The ratio of settlement to pile diameter was  $s/D = 0.0049$  related to total settlements. The measurement results have shown that a base resistance of  $q_b = 122 \text{ kN/m}^2$  (equates to 216 kN) occurred at the maximum load stage. The average skin friction within sand layers (P-al) and gravel layers (S-al) and marl (M) was approx.  $q_s = 56 \text{ kN/m}^2$ .

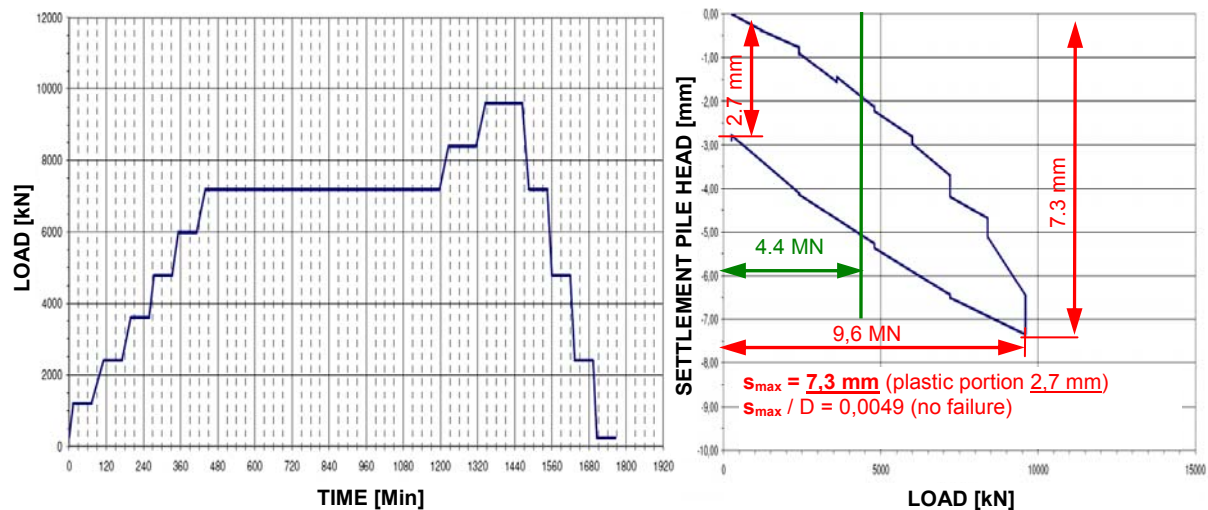


**Figure 26.** Results of axial static pile load test at Pier 6; maximum test load of 9.6 MN with a maximum working load of 4.4 MN (Bauer Spezialtiefbau GmbH, 2009).

By means of measurement results (particularly with regard to measured deformation) it could be assumed that the ultimate limit state was not reached with the test load of 9.6 MN. This means, that the bearing capacity had to be higher than the test load. Hence, testing results were better than expected. Due to rock-similar behaviour of marls skin friction within layers P-al and S-al (both granular soil) was not mobilised, because of low vertical deformations. Although the ultimate bearing capacity of base resistance and skin friction of each single layer could not be determined by pile load tests, it was proven that the intended workloads could be transferred to the ground with low deformations and sufficient safety. Thus, design parameters (Geotechnik Adam ZT GmbH, 2009) were approved and could be used for designing the pile foundations. Finally, the results of these trial piles provided also information about the settlements of a single pile and were applied for settlement calculations.

### 3.6. Settlements

Foundations were designed for the serviceability limit state (SLS) as well so that calculated settlements met the requirements derived from the allowable deformations of the superstructure. According to Brandl (2005) for settlement analyses the monolith-theory has proved practicable and sufficiently accurate in engineering practice by assuming the base of the box-foundation as the fictitious surface in the half space. The theoretical contact pressure includes the reduction of the total load  $Q$  by the shaft friction  $Q_s$ .

In the static model of the superstructure a stiffness matrix was integrated at each pier in order to consider the pile foundation. Furthermore, additional differential settlement  $\Delta s$  with  $\pm 1.0$  cm ( $|\Delta s| = 2.0$  cm) was considered at each support using the elastic stiffness of the structure, whereas at the pylon axis a settlement  $\Delta s$  of 5.0 cm and a rotation  $\Delta\varphi$  of  $\pm 1.0\%$  were considered. Due to ground conditions at Piers 7 and 8 (rock) and the results of trial piles differential settlement  $\Delta s$  with  $\pm 0.5$  cm ( $|\Delta s| = 1.0$  cm) was assumed for the axis 7 and 8.

In order to check the assumptions settlement calculations with the static model of the superstructure have been performed. The foundation of the piers is within rock-like marl at Piers 1 to 6 and within sandstone at Piers 7 and 8. Therefore, the piles predominantly work as end bearing piles. The total settlements ( $s_{total}$ ) of the foundation consist of the settlements of the single piles ( $s_1$ ) as well as the settlements of the pile group ( $s_2$ ) (DIN 1054, 2005):

$$s_{total} = s_1 + s_2$$

The settlements of a single pile were derived from pile load tests (trial piles) taking into account the maximum working load of a single pile. For settlement calculations of the pile group the envelope area of all piles (resp. diaphragm walls at pier 6) in the foundation depth was taken as a basis. For this quasi-monolith the settlement calculations were performed like a shallow foundation with a deep foundation level (e.g. according to DIN 4019). The total load was distributed over the total base of this quasi-monolith. The overburden stress in the foundation depth was then compared with the additional stress due to the bridge loads. The thickness of the compressible layer was limited to a depth (limit depth), where the additional stress reached 20% of the overburden stress.

Settlement calculations were performed with working loads without safety factors. Therefore, separate static calculations were carried out neglecting any safety factor in order to calculate working loads of each pile.

At Pier 6 (pylon axis) an average stress of 581 kN/m<sup>2</sup> was expected in the foundation depth. The additional stress of 39.6 kN/m<sup>2</sup> due to the dead load of concrete elements (piles, diaphragm wall, pile raft) had to be added, so that the total additional stress for settlement calculation amounted to 620 kN/m<sup>2</sup>.

Depending on the modulus of compression for the marl and the limestone (beneath marl) the settlements of foundation were estimated to

$$s_2 = 3.0 \text{ cm to } 4.0 \text{ cm}$$

with a limit depth of 70.3 m. With an estimated settlement of the single pile

$$s_1 = 0.5 \text{ cm}$$

the total settlements for final stage amounted to

$$s_{total} = s_1 + s_2 = 3.5 \text{ cm to } 4.5 \text{ cm}$$

Differential settlements of the pier foundation due to load distribution within the pile group could be derived from settlement calculations of the box-shaped foundation and were estimated to  $\Delta s \leq 0.5$  cm.

Regarding the rotation of the pier foundation several calculations were performed in order to consider load distribution, inclined rock surfaces in longitudinal and transversal directions and varying soil /rock modulus. Due to the results it was recommended to set a rotation of 1‰ for the pier foundation in the static model.

The settlement calculations for final stage (see Table 13) have shown that the settlements of Pier 1 are less than the settlements of the other piers, because of lower load from superstructure at this pier. The same conditions occur at Pier 5: due to the cables a part of the load from superstructure is transferred to Pier 6, which results in a minor foundation load at Pier 5.

Piers 1 to 6 are founded within marl. However, at Pier 6 the settlements are relatively low, although the total load is high in comparison to the other piers. The reason is that at Pier 6 the limestone (rock) is only a few meters below foundation level. The limestone was considered only at Pier 6 in the settlement calculations, because the interface was explored only in exploratory drillings at Pier 6.

However, for the superstructure the differential settlements shown in Table 13 are not relevant, because construction stages and settlements, which have already occurred until bearings for superstructure are installed, were not considered. Therefore, additional settlement calculations for the following construction stages have been performed:

- Construction stage A: Start of construction works
- Construction stage B: Completion of pier construction
- Construction stage C: Launching of superstructure is finished
- Final stage

Only settlements and in particular differential settlements which occur after construction stage C influence the superstructure, because bridge bearings are installed just before this construction stage. However, these calculations have shown that the assumptions for the static model of superstructure are on the safe side and that the expected differential settlements are lower than those considered in the static calculation of the superstructure.

**Table 13:** Predicted and allowable settlements at final stage and differential settlements after pier construction.

PIER	PREDICTED SETTLEMENTS AT FINAL STAGE $s_{total} = s_1 + s_2$	DIFFERENTIAL SETTLEMENTS AFTER PIER CONSTRUCTION	
		$\Delta s_{predicted}$	$\Delta s_{allowable (superstructure)}$
Pier 1	1,5 – 2,5 cm	2,0 – 2,5 cm	2,7 cm
Pier 2	4,0 – 5,0 cm	0,5 – 1,0 cm	2,1 cm
Pier 3	3,5 – 4,5 cm	0,5 – 1,0 cm	2,4 cm
Pier 4	2,5 – 3,5 cm	1,0 – 1,5 cm	2,4 cm
Pier 5	2,0 – 3,0 cm	<b>2,0 – 2,5 cm</b>	<b>5,4 cm</b>
<b>Pier 6</b>	<b>3,5 – 4,5 cm</b>	<b>3,0 – 3,5 cm</b>	<b>7,1 cm</b>
Pier 7	0,0 – 1,0 cm	0,0 – 0,5 cm	1,2 cm
Pier 8	0,0 – 1,0 cm		

Hitherto settlement measurements indicate that real settlements most probably will not exceed the predicted settlements.

### 3.7. Foundation Construction Works

Foundation works started in summer 2008. The deep foundation works for all piers and auxiliary foundations for launching could be finished within the defined time schedule.



**Figure 27.** Main construction sequences of deep foundation works for box-shaped foundation at Pier 6 on man-made working platform at Ada Ciganlija Island (construction of diaphragm walls and piles, removal of pile heads after concreting, placing of blinding layer, reinforcement works, construction of pile raft, scaffolding and formwork for pylon).

Construction for the foundation and the pylon of Pier 6 took place on a man-made peninsula at Ada Ciganlija Island (see Figure 27), which was filled prior to the bridge construction. The exceptional challenge for the foundation works was the access situation, which had to be accomplished with barks, ferries and boats since Ada Ciganlija Island was dedicated an environmental protection and recreation area of the City of Belgrade. Consequently, all the earth and foundation works and in particular the concreting phases for the diaphragm wall, the piles and the pile raft had to be planned carefully in advance since concrete had to be delivered just in time. In

peak periods up to 400 m<sup>3</sup> of concrete were required, which were transported with barks to the man-made construction platform. Three modern crawler type carrier machines (one Liebherr HS875 and two HS855) and a powerful large diameter drilling machinery (Bauer BG 40) were applied in parallel in order to complete the entire deep foundation works at Pier 6 within 12 weeks only (Hinterplattner et al., 2011).



**Figure 28.** Sava Bridge building construction in progress (January 2011) and visualisation of the completed bridge, the new spectacular landmark of Belgrade.

#### **4. COMPARISON OF THREE DIFFERENT FOUNDATION CONCEPTS**

Finally, the three different foundation concepts are compared and discussed. Ground improvement facilitates primarily a homogenization of ground conditions, an increase of the bearing capacity and in many cases an acceleration of consolidation settlements but it is not the primary target to reduce settlements to a minimum. Hybrid foundation is a combination of ground improvement during installation works and of its deep foundation behaviour after accomplishment by one and the same technique, thus, providing both better ground conditions and transfer of (high) loads deeply into the ground. Deep foundation either bridges unfavourable ground layers to good bearing soil or rock layers or transfers (very high) loads deeply into the ground, thus, avoiding major settlements.

In the following figures the concepts are faced and it is illustrated that all the concepts are justified taking into account the ground conditions, structural and serviceability requirements of the buildings, and economical factors (time and cost). Depending on the ground conditions and the function with respect to bearing behaviour and deformation behaviour (serviceability) each concepts exhibits advantages and benefits.

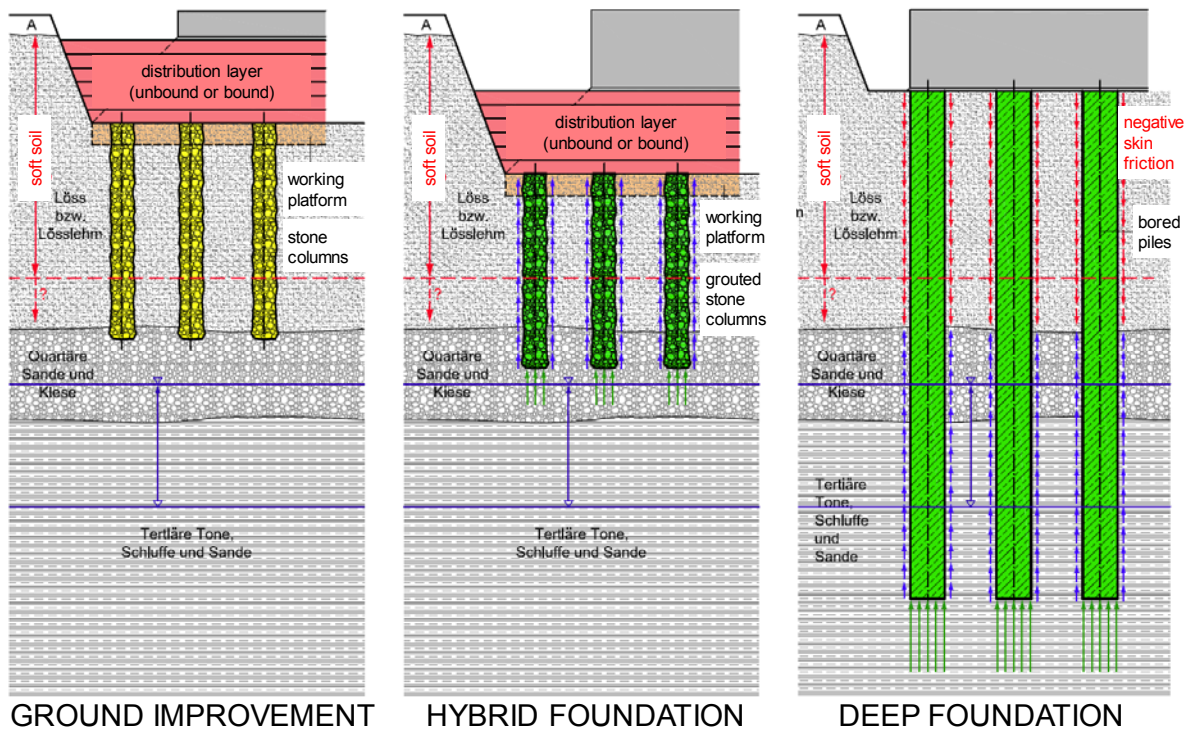


Figure 29. Comparison of foundation concepts

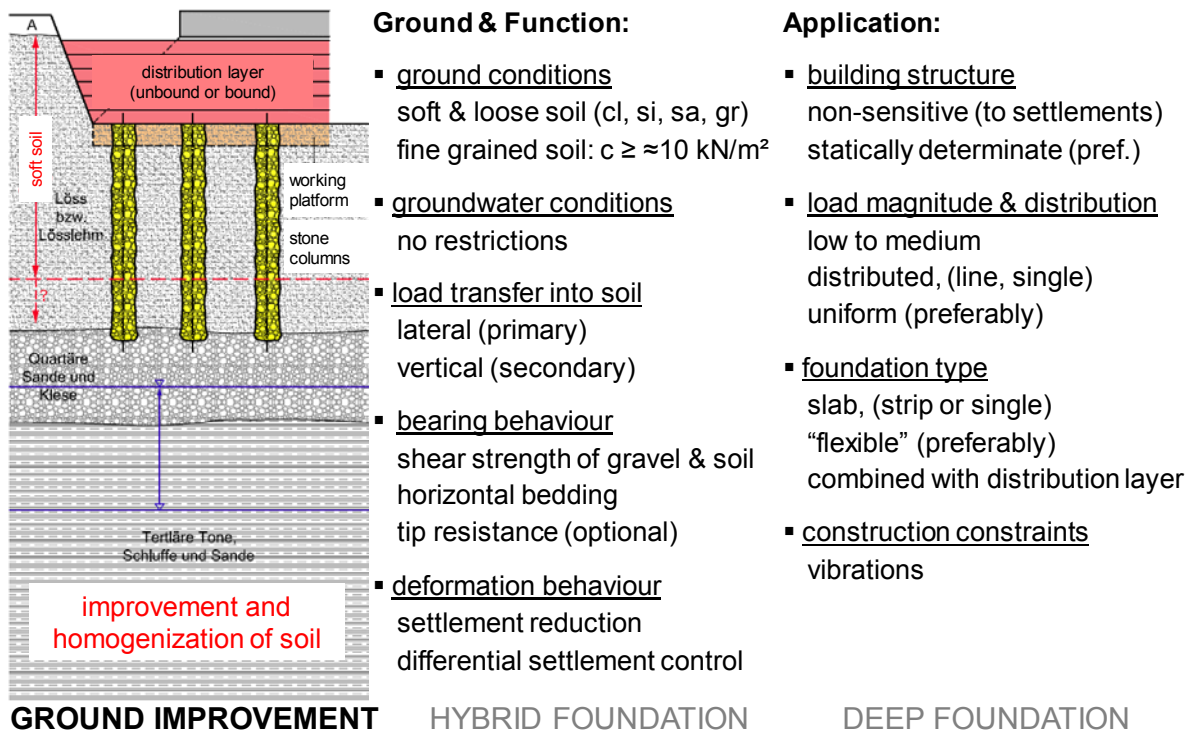
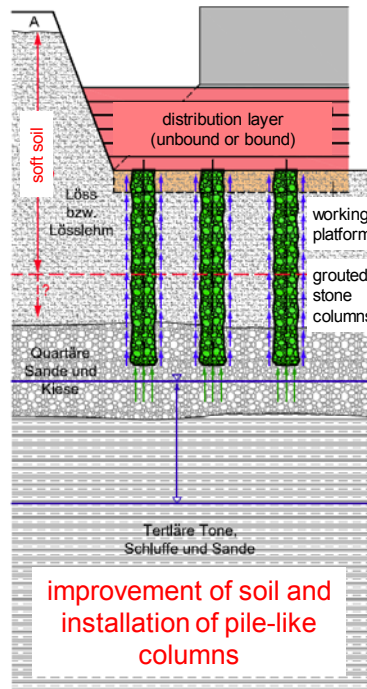


Figure 30. Ground improvement

**Ground & Function:**

- ground conditions  
soft & loose soil (cl, si, sa, gr)  
collapsible soil (!)
- groundwater conditions  
no restrictions
- load transfer into soil  
lateral (after installation)  
vertical (after hydration)
- bearing behaviour  
material compressive strength  
skin friction (improved soil)  
tip resistance (optional)
- deformation behaviour  
medium to low settlements  
low differential settlements

GROUND IMPROVEMENT



HYBRID FOUNDATION

**Application:**

- building structure  
sensitive (to settlements)  
statically (in)determinate
- load magnitude & distribution  
medium to high  
single, line & distributed  
uniform to irregular
- foundation type  
slab, strip or single  
“flexible” or “rigid”  
combined with distribution layer
- construction constraints  
vibrations

DEEP FOUNDATION

Figure 31. Hybrid foundation

**Ground & Function:**

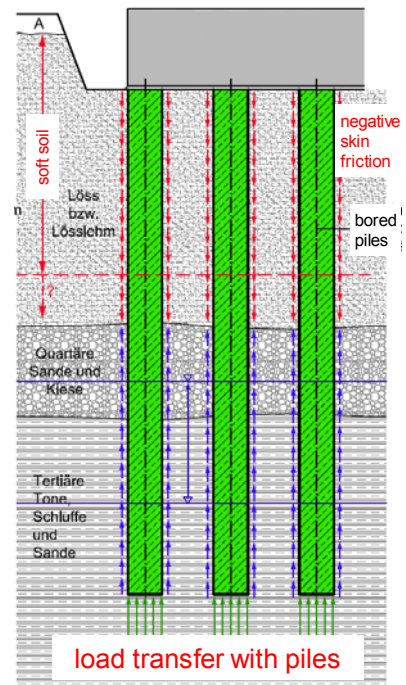
- ground conditions  
soil & rock (any)
- groundwater conditions  
no restrictions (pile install.)
- load transfer into soil  
vertical (horizontal, bending)  
(floating piles – end bearing p.)
- bearing behaviour  
pile compressive strength  
skin friction (floating)  
tip resistance (end bearing)
- deformation behaviour  
settlement minimization  
differential settlement  
minimization

GROUND IMPROVEMENT

**Application:**

- building structure  
very sensitive (to settlements)  
statically indeterminate (pref.)
- load magnitude & distribution  
high to very high  
single, line & distributed  
uniform to irregular
- foundation type  
slab, strip or single (any)  
capping beams etc.  
highly reinforced  
“rigid”
- construction constraints  
depending on pile type and  
piling system

HYBRID FOUNDATION



DEEP FOUNDATION

Figure 32. Deep foundation

## 5. CONCLUSIONS

In the first chapter the ground improvement concept and in particular the settlement behaviour of the new stadium in Klagenfurt is presented which was built from 2006 to 2007 for the European Soccer Championship EURO 2008. Due to the unfavourable soil conditions consisting of unconsolidated lake deposits underlain by moraine and the bed rock in varying depth large settlements were predicted and significant differential settlements were expected due to non-uniform loads which had to be taken into account for compatibility requirements between adjacent structural elements. Ground conditions were improved and homogenized up to 18 m by installing stone columns using the vibro replacement technique. Long-term monitoring of settlements and a well instrumented field trial have been carried to document the time-dependent settlement process and to investigate the performance of the floating stone column foundation. Back analysis using the Soft Soil Creep model (SSC) was performed to calculate the settlement process and final settlements. Results compare well with measurements from the extensometer and agree with measured settlements of the foundation slab at the west side. Agreement on the east side is less satisfactory and one possible reason for this could be that the load has been overestimated in this part of the foundation.

In the second chapter the innovative hybrid foundation concept of CCCP Malženice is presented. The foundation measures for the 400 MW gas fired combined cycle power plant at Malženice, in the western part of Slovakia, constructed by E.ON Elektrárne, s.r.o., the in Trakovice based subsidiary of E.ON Kraftwerke GmbH in Hannover, Germany, comprise deep soil improvement and deep foundation elements (hybride foundation), and soil stabilization. The hybrid foundation is realized by the grouted stone columns (pile-like bearing elements) embedded within the gravel layer complex produced using the deep vibro replacement technique and deep improvement of the soil around the columns due to the vibration process (anticipation of collapse in the soil structure and compaction). The working platform, stabilized by the mixed-in-place method with a lime-cement binder (KZM), ensured the deep improvement and deep compaction. The filling above the columns up to the level of the blinding layer has also been stabilized with KZM. The presented innovative hybrid foundation concept supervised by an extensive quality control programme is being executed alternatively to the original foundation concept. Thus, significantly shorter deep foundation elements in comparison with piles according to the original foundation concept could be realized.

In the third chapter the deep foundation concept of the new cable-stayed bridge over the Sava River in Belgrade near entry of the Sava into the River Danube is presented. The foundation at 8 piers for the new bridge over the Sava River in Belgrade was successfully accomplished based on an innovative design procedure according to EC 7. The Sava Bridge is the first execution of EC 7 using the national application rules of Austria for pile foundations of a major bridge. In conclusion the foundations were economically designed in such a way that they have both sufficiently high global safety against failure and also sufficiently high safety in the serviceability limit state, thus, considering the behaviour during life time. All the bridge foundations show satisfactory settlement behaviour already during construction and after completion. The bridge is the new landmark of Belgrade; nevertheless the deep foundations are invisible but will provide a safe basis for the lifetime of the new Sava Bridge.

When comparing the different foundation concepts in conclusion no ranking can be done with respect to the issue, which is the best concept. All of them are justified taking into account the ground conditions, structural and serviceability requirements of the buildings, and economical factors (time and cost) as well.

## REFERENCES

- Adam D., Geotechnik Adam ZT GmbH. (2008a) Geotechnical Report for the Construction of a 400 MW Combined Cycle Power Plant (CCPP) in SK 91929 Malzenice, Slovakia (in German): A-2345 Brunn am Gebirge, Wiener Straße 66-72/15/4; (unpublished).
- Adam D., Geotechnik Adam ZT GmbH. (2008b). Quality control plan for the foundation works (in German). A-2345 Brunn am Gebirge, Wiener Straße 66-72/15/4; (unpublished).
- Adam, D., Geotechnik Adam ZT GmbH (2008c). Wörthersee-Stadion Klagenfurt, Gründungsarbeiten, Geotechnischer Schlussbericht. A-2345 Brunn am Gebirge, Austria.
- Adam, D., Markiewicz, R. (2011): *A new spectacular bridge over the Sava River in Belgrade – foundation design and construction*. In: Proc. of 10<sup>th</sup> International Geotechnical Conference, Slovak University of Technology Bratislava, Faculty of Civil Engineering, Department of Geotechnics, 30 – 31 May 2011, p. 176-195, Bratislava, Slovakia.
- Adam, D., Schweiger, H.F., Markiewicz, R., Knabe, T. (2010): *EURO 2008 Stadium Klagenfurt – Prediction, Monitoring and Back Calculation of Settlement Behaviour*. In: Proc. of the XIV<sup>th</sup> Danube-European Conference on Geotechnical Engineering „From Research to Design in European Practice“, 2 – 4 June 2010, Bratislava, Slovakia.
- Adam, D., Turcek, P., Paulmichl, I. (2009): *Innovative hybrid ground improvement and deep foundation concept for the CCPP Malženice (Slovakia)*. In: Proc. of 9<sup>th</sup> International Geotechnical Conference, Slovak University of Technology Bratislava, Faculty of Civil Engineering, Department of Geotechnics, 1 – 2 June 2009, p. 59-68, Bratislava, Slovakia.
- Bauer Spezialtiefbau GmbH (2009): Belgrad Sava Bridge, Pfahlprobelastung, Bericht Nr. 04/02/09. February 2, 2009, unpublished.
- Bautechnische Versuchs- und Forschungsanstalt Salzburg (2006). Prüfbericht, Baugrunderkundung, Probefeld Stadion Klagenfurt. A-5020 Salzburg, Austria.
- Bjerrum, L. (1967). Engineering geology of Norwegian normally-consolidated marine clays as related to settlements of buildings. Seventh Rankine Lecture. Géotechnique, 17:81-118.
- Brandl, H. (2003): Box-shaped foundations of bored and auger piles (or diaphragm walls). Proceedings of the 4th International Geotechnical Seminar on Deep Foundations on Bored and Auger Piles. Millpress Rotterdam. Ghent.
- Brandl, H. (2005): Settlement-Minimizing pile and diaphragm wall foundations for high rise buildings and bridges. Geotechnics in urban areas. Bratislava, June 27-28, 2005.
- Brinkgreve, R.B.J., Broere, W. & Waterman, D. (2006). Plaxis, Finite element code for soil and rock analyses, user's manual. The Netherlands.
- DIN 1054 (2005): Subsoil – Verification of the safety of earthworks and foundations.
- Fross, M., Adam, D., Hofmann, R. (2010): Pile Foundations for River Bridges according to EC 7-1. Proc. of the XIV<sup>th</sup> Danube-European Conference on

Geotechnical Engineering, From Research to Design in European Practice, 2 – 4 June 2010, Bratislava, Slovakia.

Gäb, M., Schweiger, H.F., Thurner, R., Adam, D. (2007): Field trial to investigate the performance of a floating stone column foundation (in coop. with). In: Proc. of XIV European Conference on Soil Mechanics and Geotechnical Engineering (XIV ECSMGE), Madrid, Spain, p. 1311 – 1316.

Gäb M., Schweiger H.F., Kamrat-Pietraszwska D. and Karstunen M. (2008). Numerical analysis of a floating stone column foundation using different constitutive models. In Karstunen and Leoni, Geotechnics of Soft Soils, volume 1, 137-142.

Geotechnik Adam ZT GmbH (2009): Geotechnical Interpretive Report for the Bridge over the River Sava – Trial Piles. February 26, 2009, (unpublished).

Geotechnik Adam ZT GmbH (2009): Geotechnical Interpretive Report for the Bridge over the River Sava – Piers 1 to 7. Revision B. April 30, 2009, (unpublished).

Geotechnik Adam ZT GmbH (2009): Settlement Report for the Bridge over the River Sava – Piers 1 to 8. July 29, 2009, (unpublished).

Hinterplattner, B., Markiewicz, R., Adam, D. (2011): Sava Bridge Belgrad – Eine innovative Pylonfundierung für eine spektakuläre Schrägseilbrücke. 8. Österreichische Geotechniktagung 03.-04.02.2011, Wien.

[http://www.eon-elektrarne.com/pages/ekw\\_en/index.htm](http://www.eon-elektrarne.com/pages/ekw_en/index.htm)

Ingenieurgesellschaft Garber & Dalmatiner Zivilingenieure (2005a). Bodenmechanisches Gutachten zum Projekt Wörthersee-Stadion Klagenfurt, Neubau. A-8010 Graz bzw. A-9500 Villach, Austria.

Ingenieurgesellschaft Garber & Dalmatiner Zivilingenieure (2005b). Ergänzung zum bodenmechanischen Gutachten zum Projekt Sportpark Wörthersee, Stadion EURO 2008, Klagenfurt. A-8010 Graz bzw. A-9500 Villach, Austria.

Janbu, N. (1967). The resistant concept applied to soils, Géotechnique 17: 81-118.

ÖNORM B 1997-1-1 (2007): Geotechnical design, General rules – National specifications concerning ÖNORM EN 1997-1 and national supplements.

ÖNORM B 1997-1-3 (2007), draft version: Berechnung und Bemessung in der Geotechnik – Pfahlgründungen, Ermittlung der Tragfähigkeit (in German).

ÖNORM B 4440 (2001): Erd- und Grundbau, Großbohrpfähle, Tragfähigkeit (in German).

ÖNORM B 4431-2. (1986). Geotechnical engineering; permissible soil pressures; settlement observations.

ÖNORM EN 1997-1 (EC 7) (2006): Geotechnical design, General rules.

Steinkühler M. et al. (2010): Ein neues Wahrzeichenzeichen für Belgrad: Schrägseilbrücke mit 200 m Pylon über die Sava in Belgrad, Serbien. Betontag 22.-23.04.2010, ÖVBB, Wien.

Vermeer P. and Neher, H. (2000). A soft soil model which accounts for creep. Beyond 2000 in Computational Geomechanics - 10 years of PLAXIS International, Balkema.